J|A|C|S ARTICLES

Published on Web 07/12/2010

Dehydrogenation of Saturated CC and BN Bonds at Cationic N-Heterocyclic Carbene Stabilized M(III) Centers (M = Rh, Ir)

Christina Y. Tang, Amber L. Thompson, and Simon Aldridge*

Inorganic Chemistry Laboratory, Department of Chemistry, University of Oxford, South Parks Road, Oxford OX1 3QR, U.K.

Received May 20, 2010; E-mail: simon.aldridge@chem.ox.ac.uk

Abstract: Chloride abstraction from the group 9 metal bis(N-heterocyclic carbene) complexes $M(NHC)_2(H)_2Cl$ [M = Rh, Ir; NHC = IPr = *N*,*N*′-bis(2,6-diisopropylphenyl)imidazol-2-ylidene or IMes = *N*,*N*′-bis(2,4,6-trimethylphenyl)imidazol-2-ylidene] leads to the formation of highly reactive cationic species capable of the dehydrogenation of saturated CC and BN linkages. Thus, the reaction of $Ir(IPr)_2(H)_2Cl$ (**1**) with $Na[BAr^f_4]$ in fluorobenzene generates $[Ir(IPr)_2(H)_2]^+[BAr^f_4]^-$ (**4**) in which the iridium center is stabilized by a pair of agostic interactions utilizing the methyl groups of the isopropyl substituents. After a prolonged reaction period C−H activation occurs, ultimately leading to the dehydrogenation of one of the carbene ^{i}Pr substituents and the formation of $[Ir(IPr)(IPr'')(H)_2]^+[BAr^f_4]^-$ (**5**), featuring the mixed NHC/alkene donor IPr″ ligand. By contrast, the related IMes complexes $M(IMes)_2(H)_2Cl$ (M = Rh, Ir), which feature carbene substituents lacking β-hydrogens, react with $Na[BAr^f_4]$ in fluorobenzene to give rare examples of NaCl inclusion compounds, viz., $[M(IMes)_2(H)_2Cl(Na)]^+[BAr^f_4]^-$ (M = Rh, **6**; M = Ir, **7**). Intercalation of the sodium cation between the mesityl aromatic rings of the two NHC donors has been demonstrated by crystallographic studies of **7**. Synthetically, **6** and **7** represent convenient yet highly reactive sources of the putative 14-electron $[M(NHC)_2(H)_2]^+$ cations, readily eliminating NaCl in the presence of potential donors. Thus **7** can be employed in the synthesis of the dinitrogen complexes $[Ir(IMes)_2(N_2)_2]^+[BAr^f_4]^-$ (**8a**) and $[Ir(IMes)_2(N_2)THF]^+[BAr^f_4]^-$ (**8b**) (albeit with additional loss of H_2) by stirring in toluene under a dinitrogen atmosphere and recrystallization from the appropriate solvent system. The interactions of **6** and **7** with primary, secondary, and tertiary amineboranes have also been investigated. Although reaction with the latter class of reagent simply leads to coordination of the amineborane at the metal center via two M−H−B bridges {and formation, for example, of the 18-electron species $[M(IMes)_2(H)_2(\mu\text{-}H)_2B(H)\cdot NMe_3]^+[BAr^f_4]^-$ (M = Rh, **9**; M = Ir, **10**)}, the corresponding reactions with systems containing N−H bonds proceed via dehydrogenation of the BN moiety to give complexes containing unsaturated aminoborane ligands. Thus, for example, **6** catalyzes the dehydrogenation of $R_2NH\cdot BH_3$ (R = ^{i}Pr, Cy) in fluorobenzene solution (100% conversion over 6 h at 2 mol % loading) to give R_2NBH_2; the organometallic complex isolated at the end of the catalytic run in each case is shown to be $[Rh(IMes)_2(H)_2(\mu\text{-}H)_2BNR_2]^+[BAr^f_4]^-$ (R = ^{i}Pr, **11**; R = Cy, **12**). In contrast to isoelectronic alkene donors, the aminoborane ligand in these complexes (and in the corresponding iridium compounds **13** and **14**) can be shown by crystallographic methods to bind in end-on fashion via a bis(σ-borane) motif. Similar dehydrogenation chemistry is applicable to the primary amineborane ^{t}BuNH$_2\cdot$BH$_3$, although in this case the *rate* of rhodium-catalyzed dehydrogenation is markedly slower. This enables the amineborane complex $[Rh(IMes)_2(H)_2(\mu\text{-}H)_2B(H)\cdot NH_2{}^tBu]^+[BAr^f_4]^-$ (**15**) to be isolated at short reaction times (ca. 6 h) and the corresponding (dehydrogenated) aminoborane system $[Rh(IMes)_2(H)_2(\mu\text{-}H)_2BNH{}^tBu]^+[BAr^f_4]^-$ (**16**) to be isolated after an extended period (ca. 48 h). As far as further reactivity is concerned, aminoborane systems such as **14** show themselves to be amenable to further dehydrogenation chemistry in the presence of *tert*-butylethylene leading ultimately to the dehydrogenation of the boron-containing ligand and to the formation of a directly Ir−B bonded system described by limiting boryl (Ir−B) and borylene (Ir═B) forms.

Introduction

Electron-deficient late transition metal complexes stabilized, for example, by labile intramolecular agostic or intermolecular solvent molecule/counterion derived interactions[1−4] have been implicated in the coordination or activation of a range of chemical bonds and, in favorable cases, exploited in catalytic processes for the functionalization of simple organic/inorganic molecules.[5−7] Within this area, low electron count complexes of rhodium and iridium have been the subject of significant interest, having been shown to be effective in both alkane dehydrogenation and alkene hydrogenation chemistries.[8,9]

(1) For reviews of agostic interactions see, for example: (a) Brookhart, M.; Green, M. L. H. *J. Organomet. Chem.* **1983**, *250*, 395–408. (b) Brookhart, M.; Green, M. L. H.; Wong, L.-L. *Prog. Inorg. Chem.* **1988**, *36*, 1–124. (c) Crabtree, R. H. *Angew. Chem., Int. Ed. Engl.* **1993**, *32*, 789–805. (d) Brookhart, M.; Green, M. L. H.; Parkin, G. *Proc. Natl. Acad. Sci. U.S.A.* **2007**, *104*, 6908–6914.

(2) For reviews of weakly coordinating anions see, for example: Strauss, S. H. *Chem. Rev.* **1993**, *93*, 927–942. (b) crossing, I.; Raabe, I. *Angew. Chem., Int. Ed.* **2004**, *43*, 2066–2090. (c) Koerbe, S.; Schreiber, P. J.; Michl, J. *Chem. Rev.* **2006**, *106*, 5208–5249. (d) Reed, C. A. *Acc. Chem. Res.* **2010**, *43*, 121–128.

10.1021/ja1043787

Highly unsaturated Rh(I) and Ir(I) complexes, both cationic and charge-neutral, are often prone to side reactions involving oxidative addition of ancillary C−H bonds;[10] systems bearing β-hydrogen atoms offer the additional possibility for further steps leading to ligand dehydrogenation.[11−14] The greater resistance to oxidative addition of M(III) complexes, however,[5,15] means that 14-electron systems of the type $[(R_3P)_2M(H)_2]^+$, stabilized by secondary agostic interactions, are accessible from related charge-neutral systems via halide abstraction; subsequently, such systems have been exploited in a number of a catalytic dehydrogenation processes.[10b,c,16] In recent work we have been targeting analogous bis(NHC) ligated systems in the hope of exploiting the very strong σ donor properties of the NHC ligand class to stabilize M(III) complexes of the type $[(NHC)_2M(H)_2]^+$ (M = Rh, Ir).[17,18] A primary aim of this work at the outset was the exploitation of such highly electrophilic systems in the trapping of reactive species such as those generated in the dehydrogenation of amineboranes.

The metal-catalyzed dehydrogenation of ammonia borane (AB, $H_3N{\cdot}BH_3$) and related primary and secondary amine derivatives ($RH_2N{\cdot}BH_3$ and $R_2HN{\cdot}BH_3$) has been the subject of significant recent interest, both with an ultimate aim of unlocking the potential of such systems as hydrogen storage media and with a view to developing new Group 13/15 materials by dehydrocoupling approaches.[19−21] Typically, in the absence of significant steric bulk at R, the dehydrogenation of alkyl- or dialkyl-amineboranes catalyzed by Group 9 metal systems leads to the formation of oligo- or polymeric products.[20] The implication of metal complexes containing the unsaturated aminoborane unit [i.e., $L_nM(H_2BNR_2)$] in such processes has been debated, but until recent preliminary reports by us and by Sabo-Etienne,[17,22] the structural characterization of these systems had remained elusive. In targeting such complexes, the monomeric nature of R_2NBH_2 (R = ^{i}Pr, Cy)[23,24] led us to consider the in situ rhodium- or iridium-catalyzed dehydrogenation of $^i Pr_2HN{\cdot}BH_3$ and $Cy_2HN{\cdot}BH_3$ as a potential synthetic approach.

(3) For a review of halocarbon coordination see, for example: (a) Kulawiec, R. J.; Crabtree, R. H. *Coord. Chem. Rev.* **1990**, *99*, 89–115.

(4) For solvent-stabilized systems relevant to the current study see, for example: (a) Crabtree, R. H.; Hlatky, G. G.; Parnell, C. P.; Segmüller, B. E.; Uriate, R. J. *Inorg. Chem.* **1984**, *23*, 354–358. (b) Burk, M. J.; Segmüller, B.; Crabtree, R. H. *Organometallics* **1987**, *6*, 2241–2246. (c) Luo, X.-L.; Schulte, G. K.; Crabtree, R. H. *Inorg. Chem.* **1990**, *29*, 682–686. (d) He, X. D.; Fernandez-Baeza, J.; Chaudret, B.; Felting, K.; Caulton, K. G. *Inorg. Chem.* **1990**, *29*, 5000–5002. (e) Dahlenberg, L.; Menzel, R.; Heinemann, F. W. *Acta Crystallogr.* **2007**, *E63*, m2769–m2770. (f) Ingelson, M.; Brayshaw, S. K.; Mahon, M. F.; Ruggiero, G. D.; Weller, A. S. *Inorg. Chem.* **2005**, *44*, 3162–3171. (g) Gandelman, M.; Konstantinovski, L.; Rozenberg, H.; Millstein, D. *Chem.−Eur. J.* **2003**, *9*, 2595–2602. (h) Moxham, G. L.; Brayshaw, S. K.; Weller, A. S. *Dalton Trans.* **2007**, 1759–1761.

(5) (a) Collman, J. P.; Hegedus, L. S.; Norton, J. R.; Finke, R. G. In *Principles and Applications of Organotransition Metal Chemistry*; University Science Books: Sausalito, CA, 1987;.(b) Hartwig, J. F. In *Organotransition Metal Chemistry*; University Science Books: Sausalito, CA, 2010.

(6) Herrmann, W. A.; Cornils, B. *Angew. Chem., Int. Ed. Engl.* **1997**, *36*, 1048–1067.

(7) For selected reviews relating to H−H and C−H activation, see: (a) Crabtree, R. H. *Acc. Chem. Res.* **1990**, *23*, 95–101. (b) Zassinovich, G.; Mestroni, G.; Gladiali, S. *Chem. Rev.* **1992**, *92*, 1051–1069. (c) Arndtsen, B. A.; Bergman, R. A.; Mobley, T. A.; Peterson, T. H. *Acc. Chem. Res.* **1995**, *28*, 154–162. (d) Stahl, S. S.; Labinger, J. A.; Bercaw, J. E. *Angew. Chem., Int. Ed.* **1998**, *37*, 2181–2192. (e) Labinger, J. A.; Bercaw, J. E. *Nature* **2002**, *417*, 507–514. (f) Crabtree, R. H. *J. Organomet. Chem.* **2004**, *689*, 4083–4091. (g) Klei, S. R.; Tan, K. L.; Golden, J. T.; Yung, C. M.; Thalji, R. K.; Ahrendt, K. A.; Ellman, J. A.; Tilley, T. D.; Bergman, R. G. *ACS Symp. Ser.* **2004**, *885*, 46–55. (h) Perutz, R. N.; Sabo-Etienne, S. *Angew. Chem., Int. Ed.* **2007**, *46*, 2578–2592. (i) Kubas, G. J. *Proc. Natl. Acad. Sci. U.S.A.* **2007**, *104*, 6901–6097. (j) Bercaw, J. E.; Labinger, J. A. *Proc. Natl. Acad. Sci. U.S.A.* **2007**, *104*, 6899–6900. (k) Colby, D. A.; Bergman, R. G.; Ellman, J. A. *Chem. Rev.* **2010**, *110*, 624–655. (l) Willis, M. C. *Chem. Rev.* **2010**, *110*, 725–748. (m) Mkhalid, I. A. I.; Barnard, J. H.; Marder, T. B.; Murphy, J. M.; Hartwig, J. F. *Chem. Rev.* **2010**, *110*, 890–931.

(8) See, for example: Dobereiner, G. E.; Crabtree, R. H. *Chem. Rev.* **2010**, *110*, 681–703, and references therein.

(9) See, for example: (a) Xinhua, C.; Burgess, K. *Chem. Rev.* **2005**, *105*, 3272–3296. (b) Crabtree, R. H. In *Handbook of Homogenous Hydrogenation*; De Vries, J. G., Elsevier, C. J., Eds.; Elsevier: Amsterdam, 2007.

(10) For examples relevant to the current study see: (a) Huang, J.; Stevens, E. D.; Nolan, S. P. *Organometallics* **2000**, *19*, 1194–1197. (b) Scott, N. M.; Pons, V.; Stevens, E. D.; Heinekey, D. M.; Nolan, S. P. *Angew. Chem., Int. Ed.* **2005**, *44*, 2512–2515. (c) Scott, N. M.; Dorta, R.; Stevens, E. D.; Correa, A.; Cavallo, L.; Nolan, S. P. *J. Am. Chem. Soc.* **2005**, *127*, 3516–3526.

(11) For examples of the dehydrogenation of alkyl substituents pendant to NHC ligands, see: (a) Prinz, M.; Grosche, M.; Herdtweck, E.; Herrmann, W. A. *Organometallics* **2000**, *19*, 1692. (b) Dible, B. R.; Sigman, M. S.; Arif, A. M. *Inorg. Chem.* **2005**, *44*, 3774. (c) Tang, C. Y.; Smith, W.; Vidovic, D.; Thompson, A. L.; Chaplin, A. B.; Aldridge, S. *Organometallics* **2009**, *28*, 3059–3066.

(12) For examples of the dehydrogenation of alkyl phosphines see, for example: (a) Bennett, M. A.; Clark, P. W.; Robertson, G. B.; Whimp, P. O. *J. Chem. Soc., Chem. Commun.* **1972**, 1011. (b) Hietkamp, S.; Stufkens, D. J.; Vrieze, K. *J. Organomet. Chem.* **1978**, *152*, 347. (c) Amoroso, D.; Yap, G. P. A.; Fogg, D. E. *Can. J. Chem.* **2001**, *79*, 958. (d) Six, S.; Gabor, B.; Görls, H.; Mynott, R.; Philipps, P.; Leitner, W. *Organometallics* **1999**, *18*, 3316. (e) Borowski, A. F.; Sabo-Etienne, S.; Christ, M. L.; Donnadieu, B.; Chaudret, B. *Organometallics* **1996**, *15*, 1427. (f) Deblon, S.; Liesum, L.; Harmer, J.; Schönberg, H.; Schweiger, A.; Grützmacher, H. *Chem.−Eur. J.* **2002**, *8*, 601. (g) Glaser, P. B.; Tilley, T. D. *Organometallics* **2004**, *23*, 5799. (h) Baya, M.; Buil, M. A.; Esteruelas, M. A.; Onate, E. *Organometallics* **2004**, *23*, 1416. (i) Grellier, M.; Vendier, L.; Sabo-Etienne, S. *Angew. Chem., Int. Ed.* **2005**, *46*, 2613. (j) Piras, E.; Läng, F.; Rüegger, H.; Stein, D.; Wörle, M.; Grützmacher, H. *Chem.−Eur. J.* **2006**, *12*, 5849. (k) Douglas, T. M.; Le Nôtre, J.; Brayshaw, S. K.; Frost, C. G.; Weller, A. S. *Chem. Commun.* **2006**, 3408. (l) Douglas, T. M.; Brayshaw, S. K.; Dallanegra, R.; Kociok-Köhn, G.; Macgregor, S. A.; Moxham, G. L.; Weller, A. S.; Wondimagegn, T.; Vadivelu, P. *Chem.−Eur. J.* **2008**, *14*, 1004.

(13) For examples of the dehydrogenation of alkyl substituents pendant to Nacnac and related ligand types, see: (a) Fekl, U.; Goldberg, K. I. *J. Am. Chem. Soc.* **2002**, *124*, 6804. (b) Fekl, U.; Kaminsky, W.; Goldberg, K. I. *J. Am. Chem. Soc.* **2003**, *125*, 15286. (c) Bernskoetter, W. H.; Lobkovsky, E.; Chirik, P. J. *Organometallics* **2005**, *24*, 6250. (d) Kloek, S. M.; Goldberg, K. I. *J. Am. Chem. Soc.* **2007**, *129*, 3460. (e) Giri, R.; Maugel, N.; Foxman, B. M.; Yu, J.-Q. *Organometallics* **2008**, *27*, 1667.

(14) For examples of the dehydrogenation of alkyl substituents pendant to other classes of donor ligand see, for example: (a) Yu, J. S.; Fanwick, P. E.; Rothwell, I. P. *J. Am. Chem. Soc.* **1990**, *112*, 8171. (b) Ma, Y.; Bergman, R. G. *Organometallics* **1994**, *13*, 2548. (c) Holtcampl, M. W.; Henling, L. M.; Day, M. W.; Labinger, J. A.; Bercaw, J. E. *Inorg. Chim. Acta* **1998**, *270*, 467.

(15) Gulliver, D. J.; Levason, W. *Coord. Chem. Rev.* **1982**, *46*, 1.

(16) (a) Cooper, A. C.; Streib, W. E.; Eisenstein, O.; Caulton, K. G. *J. Am. Chem. Soc.* **1997**, *119*, 9069–9070. (b) Cooper, A. C.; Clot, E.; Huffman, J. C.; Streib, W. E.; Maseras, F.; Eisenstein, O.; Caulton, K. G. *J. Am. Chem. Soc.* **1999**, *121*, 978–106. For a more recent, closely related, rhodium complex, see: (c) Douglas, T. M.; Chaplin, A. B.; Weller, A. S. *Organometallics* **2008**, *27*, 2918–2921.

(17) For a preliminary account of part of this work, see: Tang, C. Y.; Thompson, A. L.; Aldridge, S. *Angew. Chem., Int. Ed.* **2010**, *49*, 921–925.

(18) See, for example: (a) Bourissou, D.; Guerret, O.; Gabbaï, F. P.; Bertrand, G. *Chem. Rev.* **2000**, *100*, 39–92. (b) Diez-Gonzalez, S.; Marion, N.; Nolan, S. P. *Chem. Rev.* **2009**, *109*, 3612–3676.

(19) For reviews see, for example: (a) Clark, T. J.; Lee, K.; Manners, I. *Chem.−Eur. J.* **2006**, *12*, 8634–8648. (b) Marder, T. B. *Angew. Chem., Int. Ed.* **2007**, *46*, 8116–8118. (c) Stephens, F. H.; Pons, V.; Baker, R. T. *Dalton Trans.* **2007**, 2613–2626. (d) Hamilton, C. W.; Baker, R. T.; Staubitz, A.; Manners, I. *Chem. Soc. Rev.* **2009**, *38*, 279–293. (e) Smythe, N. C.; Gordon, J. C. *Eur. J. Inorg. Chem.* **2010**, 509–512.

In this article, we therefore report on the reactivity of sources of $[(NHC)_2M(H)_2]^+$ (M = Rh, Ir) toward $R_2HN\cdot BH_3$ (R = ^{i}Pr, Cy), together with comparative studies focusing on tertiary and primary amineboranes, and on ammonia borane itself. Structural characterization of a range of cationic rhodium and iridium aminoborane complexes, together with that of a closely related 1,1-disubstituted alkene complex, allows direct experimental comparison of the modes of binding of the formally isoelectronic R_2NBH_2 and R_2CCH_2 ligand systems.

Experimental Section

General Considerations. Manipulations of air-sensitive reagents were carried out under a nitrogen or argon atmosphere using standard Schlenk line or drybox techniques. With the exception of fluorobenzene (which was distilled from CaH_2), nondeuterated solvents were dried using a commercially available Braun solvent purification system. $C_6D_5CD_3$ (Goss) and 3,3-dimethyl-1-butene were degassed and dried over potassium prior to use; CD_2Cl_2 (Goss) was degassed and stored over molecular sieves. The known compounds $Na[BAr^f_4]$, $Ir(IPr)_2(H)_2Cl$ (**1**), and $M(IMes)_2(H)_2Cl$ (M = Rh, **2**; M = Ir, **3**) were prepared by literature procedures.[10a,11c,17,25] All other reagents were used as received from commercial sources. Preliminary reports of the syntheses of $[Ir(IPr)(IPr'')(H)_2]^+[BAr^f_4]^-$ (**5**), $[M(IMes)_2(H)_2Cl(Na)]^+[BAr^f_4]^-$ (M = Rh, **6**; M = Ir, **7**), $[Rh(IMes)_2(H)_2(\mu\text{-}H)_2BNR_2]^+[BAr^f_4]^-$ (R = ^{i}Pr, **11**; R = Cy, **12**); $[Ir(IMes)_2(H)_2(\mu\text{-}H)_2BN^iPr_2]^+[BAr^f_4]^-$ (**13**), and $[Rh(IMes)_2(H)_2(\mu\text{-}H)_2B(H)\cdot NH_2{}^t Bu]^+[BAr^f_4]^-$ (**15**) have been communicated by us previously.[17] NMR spectra were measured on a Varian Mercury VX-300 or Bruker AVII 500 FT-NMR spectrometer. Residual signals of solvent were used as reference for ^{1}H and ^{13}C NMR; ^{11}B and ^{19}F NMR spectra were referenced with respect to $Et_2O\cdot BF_3$ and $CFCl_3$, respectively. Infrared spectra were measured on a Nicolet 500 FT-IR spectrometer. Elemental microanalyses were carried out at London Metropolitan University. Abbreviations: br = broad, s = singlet, d = doublet, q = quartet, sept = septet, m = multiplet, IPr = *N*,*N*′-bis(2,6-diisopropylphenyl)imidazol-2-ylidene, IMes = *N*,*N*′-bis(2,4,6-trimethylphenyl)imidazol-2-ylidene, Dipp = 2,6-$^i Pr_2C_6H_3$.

Syntheses. $[Ir(IPr)_2(H)_2]^+[BAr^f_4]^-$ (4). To a suspension of $Na[BAr^f_4]$ (1.18 g, 1.33 mmol) in fluorobenzene (20 cm^3) at −30 °C was added a solution of **1** (1.34 g, 1.33 mmol) also in fluorobenzene (20 cm^3) and the reaction mixture was warmed to 20 °C over a period of 1 h. After stirring for a further 3 h at 20 °C, the resulting deep red solution was filtered and dried in vacuo, and orange crystals suitable for X-ray diffraction were obtained by concentration and storage at 0 °C. Isolated yield 1.59 g, 65%. ^{1}H NMR (C_6D_6, 500 MHz, 20 °C): δ −38.95 (s, 2H, IrH), 0.44 (d, J = 6.6 Hz, 24H, C*H*$_3$ of ^{i}Pr), 0.86 (d, J = 6.9 Hz, 24H, CH$_3$ of ^{i}Pr), 1.26 (overlapping m, 8H, CH of ^{i}Pr), 6.20 (s, 4H, NCHCHN of IPr), 6.86 (d, J = 8.1 Hz, 8H, *m*-CH of IPr), 7.16 (t, J = 6.6 Hz, *p*-CH of IPr), 7.71 (s, 4H, *p*-CH of $[BAr^f_4]^-$), 8.32 (s, 8H, *o*-CH of $[BAr^f_4]^-$). ^{13}C NMR (C_6D_6, 126 MHz, 20 °C) (i) signals due to cation: δ 23.3, 24.2 (CH$_3$ of IPr), 34.5 (CH of IPr), 122.1 (NCHCHN of IPr), 130.7 (*o*-quaternary C of IPr), 137.3 (*m*-CH of IPr), 145.1 (*p*-CH of IPr), 177.2 (br, carbene quaternary C of IPr), N-bound aryl quaternary signals not observed; (ii) signals due to anion, $[BAr^f_4]^-$: 118.0 (s, *p*-CH), 125.3 (q, J = 275.0 Hz, CF_3), 129.8 (q, J = 31.5 Hz, *m*-quaternary C), 135.6 (s, *o*-CH of anion), 162.7 (q, J = 48.0 Hz, *ipso*-quaternary C). ^{11}B NMR ($C_6D_5CD_3$, 96 MHz, 20 °C): δ −6.2. ^{19}F NMR ($C_6D_5CD_3$, 282 MHz, 20 °C): δ −61.6. IR (cm^{-1}): 2711 br [ν(agostic C−H)]. Anal. Calcd for $C_{86}H_{86}N_4IrBF_{24}$: C, 56.27; H, 4.73 N, 3.05. Found: C, 56.15; H, 4.77; N, 2.92.

$[Ir(IPr)(IPr'')(H)_2]^+[BAr^f_4]^-$ (5). To a suspension of $Na[BAr^f_4]$ (1.18 g, 1.33 mmol) in fluorobenzene (20 cm^3) at −30 °C was added a solution of **1** (1.34 g, 1.33 mmol) also in fluorobenzene (20 cm^3) and the reaction mixture was warmed to 20 °C over a period of 1 h. After further stirring for 12 h at 20 °C, the resulting deep brown solution was filtered and concentrated in vacuo, and orange crystals of **5** (as the pentane solvate) suitable for X-ray diffraction were obtained by layering with pentane and storage at 20 °C. Isolated yield: 1.89 g, 78%. ^{1}H NMR ($C_6D_5CD_3$, 300 MHz, 20 °C): δ −33.98 (s, 2H, IrH), 0.41 (d, J = 7.7 Hz, 3H, CH of ^{i}Pr), 0.85 (d, J = 7.0 Hz, 3H, CH of ^{i}Pr), 0.88 (d, J = 7.1 Hz, 12H, CH of ^{i}Pr), 1.01 (d, J = 7.9 Hz, 12H, CH of ^{i}Pr), 1.08 (d, J = 6.7 Hz, 12H, CH of ^{i}Pr), 1.15 (s, 3H, CH$_3$ of alkene), 1.25, 1.81 (br s, each 1H, CH of alkene), 2.10 (sept, J = 7.9 Hz, 2H, CH of ^{i}Pr), 2.15 (m, 1H, CH of ^{i}Pr), 2.54 (sept, J = 6.7 Hz, 2H, CH of ^{i}Pr), 3.02 (sept, J = 7.1 Hz, 2H, CH of ^{i}Pr), 6.13, 6.42, 6.84, 7.01 (s, 4H, NCHCHN of IPr and IPr''), 6.87 to 7.24 (overlapping m, 12H, aromatic CH of IPr and IPr''), 7.69 (s, 4H, *p*-CH of $[BAr^f_4]^-$), 8.40 (s, 8H, *o*-CH of $[BAr^f_4]^-$). ^{13}C NMR ($C_6D_5CD_3$, 126 MHz, 20 °C) (i) signals due to cation: δ 14.3, 22.7, 23.2, 23.3, 24.3, 25.5, 25.9, 26.7, 28.7, 28.8, 34.4, 53.1 (CH and CH$_3$ of IPr and IPr''; alkene CH$_2$ and alkene quaternary of IPr''), 123.2, 123.9, 124.2, 124.7,

(20) For Group 9-based systems see, for example: (a) Jaska, C. A.; Temple, K.; Lough, A. J.; Manners, I. *J. Am. Chem. Soc.* **2003**, *125*, 9424–9434. (b) Jaska, C. A.; Manners, I. *J. Am. Chem. Soc.* **2004**, *126*, 9776–9785. (c) Jaska, C. A.; Clark, T. J.; Clendenning, S. B.; Grozea, D.; Turak, A.; Lu, Z.-H.; Manners, I. *J. Am. Chem. Soc.* **2005**, *127*, 5116–5124. (d) Denney, M. C.; Pons, V.; Hebden, T. J.; Heinekey, D. M.; Goldberg, K. I. *J. Am. Chem. Soc.* **2006**, *128*, 12048–12049. (e) Fulton, J. L.; Linehan, J. C.; Autrey, T.; Balasubramanian, M.; Chen, Y.; Szymczak, N. K. *J. Am. Chem. Soc.* **2007**, *129*, 11936–11949. (f) Hebden, T. J.; Penney, M. C.; Pons, V.; Piccoli, P. M. B.; Koetzle, T. F.; Schulz, A. J.; Kaminsky, W.; Goldberg, K. I.; Heinekey, D. M. *J. Am. Chem. Soc.* **2008**, *130*, 10812–10820. (g) Dietrich, B. L.; Goldberg, K. I.; Heinekey, D. M.; Autrey, T.; Linehan, J. C. *Inorg. Chem.* **2008**, *47*, 8583–8585. (h) Douglas, T. M.; Chaplin, A. B.; Weller, A. S. *J. Am. Chem. Soc.* **2008**, *130*, 14432–14433. (i) Staubitz, A.; Soto, A. P.; Manners, I. *Angew. Chem., Int. Ed.* **2008**, *47*, 6212–6215. (j) Rousseau, R.; Schenter, G. K.; Fulton, J. L.; Linehan, J. C.; Engelhard, M. H.; Autry, T. *J. Am. Chem. Soc.* **2009**, *131*, 10516–10524. (k) Douglas, T. M.; Chaplin, A. B.; Weller, A. S.; Yang, X.; Hall, M. B. *J. Am. Chem. Soc.* **2009**, *131*, 15440–15456. (l) Sloan, M. E.; Clark, T. J.; Manners, I. *Inorg. Chem.* **2009**, *48*, 2429–2435. (m) Zarmakiran, M.; Özkar, S. *Inorg. Chem.* **2009**, *48*, 8955–8964. (n) Dallanegra, R.; Chaplin, A. B.; Weller, A. S. *Angew. Chem., Int. Ed.* **2009**, *48*, 6875–6878. (o) Chaplin, A. B.; Weller, A. S. *Inorg. Chem.* **2010**, *49*, 1111–1121. (p) Chaplin, A. B.; Weller, A. S. *Angew. Chem., Int. Ed.* **2010**, *49*, 581–584.

(21) For other metal systems see, for example: (a) Clark, T. J.; Russell, C. A.; Manners, I. *J. Am. Chem. Soc.* **2006**, *128*, 9582–9583. (b) Keaton, R. J.; Blacquiere, J. M.; Baker, R. T. *J. Am. Chem. Soc.* **2007**, *129*, 1844–1845. (c) Pun, D.; Lobhovsky, E.; Chirik, P. J. *Chem. Commun.* **2007**, 3297–3299. (d) Jiang, Y.; Berke, H. *Chem. Commun.* **2007**, 3571–3573. (e) Pons, V.; Baker, R. T.; Szymczak, N. K.; Heldebrant, D. J.; Linehan, J. C.; Matus, M. H.; Grant, D. J.; Dixon, D. A. *Chem. Commun.* **2008**, 6597–6599. (f) Blaquiere, N.; Diallo-Garcia, S.; Gorelsky, S. I.; Black, D. A.; Fagnou, K. *J. Am. Chem. Soc.* **2008**, *130*, 14034–14035. (g) Jiang, Y.; Blacque, O.; Fox, T.; Frech, C. M.; Berke, H. *Organometallics* **2009**, *28*, 5493–5504. (h) Friedrich, A.; Drees, M.; Schneider, S. *Chem.—Eur. J.* **2009**, *15*, 10339–10342. (i) Käss, M.; Friedrich, A.; Drees, M.; Schneider, S. *Angew. Chem., Int. Ed.* **2009**, *48*, 905–907. (j) Sloan, M. E.; Staubitz, A.; Clark, T. J.; Russell, C. A.; Lloyd-Jones, G. C.; Manners, I. *J. Am. Chem. Soc.* **2010**, *132*, 3831–3841.

(22) Alcaraz, G.; Vendier, L.; Clot, E.; Sabo-Etienne, S. *Angew. Chem., Int. Ed.* **2010**, *49*, 918–920.

(23) Pasumansky, L.; Haddenham, D.; Clary, J. W.; Fisher, G. B.; Goralski, C. T.; Singaram, B. *J. Org. Chem.* **2008**, *73*, 1898–1905.

(24) Euzenat, L.; Horhant, D.; Ribourdouille, Y.; Duriez, C.; Alcaraz, G.; Vaultier, M. *Chem. Commun.* **2003**, 2280–2281.

(25) Reger, D. L.; Wright, T. D.; Little, C. A.; Lamba, J. J. S.; Smith, M. D. *Inorg. Chem.* **2001**, *40*, 3810.

(26) (a) Cosier, J.; Glazer, A. M. *J. Appl. Crystallogr.* **1986**, *19*, 105. (b) Denzo: Otwinowski, Z.; Minor, W. *Methods in Enzymology*; Carter, C. W., Sweet, R. M., Eds.; Academic Press: New York, 1996; Vol. 276, p 307. (c) *CrystalClear (Version 2.0)*; Rigaku: Americas, TX. (d) Sir-92: Altomare, A.; Cascarano, G.; Giacovazzo, C.; Guagliardi, A.; Burla, M. C.; Polidori, G.; Camalli, M. *J. Appl. Crystallogr.* **1994**, *27*, 435. (e) CRYSTALS: Betteridge, P. W.; Carruthers, J. R.; Cooper, R. I.; Prout, J.; Watkin, D. J. *J. Appl. Crystallogr.* **2003**, *36*, 1487.

126.4, 129.2, 130.6, 135.5, 137.9, 145.1, 146.4 (NCHCHN, aromatic CH and aromatic quaternary C of IPr and IPr″), 178.2, 184.9 (carbene quaternary C of IPr and IPr″), N-bound aryl quaternary signals not observed; (ii) signals due to $[BAr^f_4]^-$ anion: 118.0 (s, *p*-CH), 124.1 (q, J = 275.0 Hz, CF_3), 129.8 (q, J = 33.1 Hz, *m*-quaternary C), 135.5 (s, *o*-CH), 162.7 (q, J = 48.0 Hz, *ipso*-quaternary C). ^{11}B NMR ($C_6D_5CD_3$, 96 MHz, 20 °C): δ −6.1. ^{19}F NMR ($C_6D_5CD_3$, 282 MHz, 20 °C): δ −61.4. Anal. Calcd for $C_{86}H_{84}N_4BF_{24}Ir$: C, 56.36; H, 3.06 N, 4.62. Found: C, 56.25; H, 3.19; N, 4.52.

$[M(IMes)_2(H)_2Cl(Na)]^+[BAr^f_4]^-$ (M = Rh, 6; M = Ir, 7). Compounds **6** and **7** were prepared by a common method given here for **7**. To a suspension of $Na[BAr^f_4]$ (1.06 g, 1.19 mmol) in fluorobenzene (20 cm^3) at −30 °C was added a solution of **2** (1.00 g, 1.19 mmol) also in fluorobenzene (20 cm^3), and the reaction mixture was warmed to 20 °C over a period of 1 h. After stirring for a further 3 h at 20 °C, the resulting deep brown solution was filtered and concentrated in vacuo, and orange crystals of **7** suitable for X-ray diffraction were obtained by layering with pentane and storage at 20 °C. Isolated yield 1.35 g, 72%. ^{1}H NMR ($C_6D_5CD_3$, 300 MHz, 20 °C): δ −34.21 (br, 2H, IrH), 1.85 (s, 24H, *o*-CH_3 of IMes), 2.13 (s, 12H, *p*-CH_3 of IMes), 5.95 (s, 4H, NCHCHN of IMes), 6.53 (s, 8H, aromatic CH of IMes), 7.64 (s, 4H, *p*-CH of $[BAr^f_4]^-$), 8.32 (s, 8H, *o*-CH of $[BAr^f_4]^-$). ^{13}C NMR ($C_6D_5CD_3$, 126 MHz, 20 °C) (i) signals due to cation: δ 19.8 (br, *o*-CH_3 of IMes), 21.3 (*p*-CH_3 of IMes), 121.5 (NCH of IMes), 124.8 (*o*-quaternary C of IMes), 127.7 (*m*-CH of IMes), 136.8 (*p*-quaternary C of IMes), 172.3 (br, carbene quaternary of IMes), N-bound aryl quaternary signal not observed; (ii) signals due to $[BAr^f_4]^-$ anion: 118.0 (s, *p*-CH), 125.2 (q, J = 273.0 Hz, CF_3), 129.9 (q, J = 30.2 Hz, *m*-quaternary C), 135.5 (s, *o*-CH), 162.6 (q, J = 50.3 Hz, *ipso*-quaternary C). ^{11}B NMR ($C_6D_5CD_3$, 96 MHz, 20 °C): δ −6.1 ($[BAr^f_4]^-$). ^{19}F NMR ($C_6D_5CD_3$, 282 MHz, 20 °C): δ −62.1. Anal. Calcd for $C_{74}H_{62}N_4ClBF_{24}NaIr$: C, 51.53; H, 3.62; N, 3.25. Found: C, 51.52; H, 3.53; N, 3.21.

Data for 6. Isolated yield 1.43 g, 68%. ^{1}H NMR ($C_6D_5CD_3$, 300 MHz, 20 °C): δ −35.24 (br, 2H, RhH), 1.93 (s, 24H, *o*-CH_3 of IMes), 2.23 (s, 12H, *p*-CH_3 of IMes), 6.19 (s, 4H, NCH of IMes), 6.70 (s, 8H, *m*-CH of IMes), 7.66 (s, 4H, *p*-CH of $[BAr^f_4]^-$), 8.32 (s, 8H, *o*-CH of $[BAr^f_4]^-$). ^{13}C NMR ($C_6D_5CD_3$, 126 MHz, 20 °C) (i) signals due to cation: δ 18.7 (br, *o*-CH_3 of IMes), 21.2 (*p*-CH_3 of IMes), 121.8 (NCH of IMes), 124.7 (*o*-quaternary C of IMes), 127.5 (*m*-CH of IMes), 136.9 (*p*-quaternary C of IMes), 177.1 (br, carbene quaternary of IMes), N-bound aryl quaternary signals not observed; (ii) signals due to $[BAr^f_4]^-$ anion: 118.1 (s, *p*-CH), 125.4 (q, J = 273.1 Hz, CF_3), 129.9 (q, J = 32.2 Hz, *m*-quaternary C), 135.5 (s, *o*-CH), 162.9 (q, J = 50.3 Hz, *ipso*-quaternary C). ^{11}B NMR ($C_6D_5CD_3$, 96 MHz, 20 °C): δ −6.2. ^{19}F NMR ($C_6D_5CD_3$, 282 MHz, 20 °C): δ −62.3. Anal. Calcd for $C_{74}H_{62}N_4BClF_{24}NaRh$: C, 54.35; H, 4.09; N, 3.43. Found: C, 54.30; H, 3.96; N, 3.51.

$[Ir(IMes)_2(N_2)L]^+[BAr^f_4]^-$ (L = N_2, 8a; L = THF, 8b). The two compounds were synthesized in closely related fashion. A sample of **7** (0.21 g, 0.125 mmol) in toluene (20 cm^3) was heated to 80 °C for 5 h under an atmosphere of dinitrogen. The resulting deep brown solution was filtered, volatiles were removed in vacuo, and the resulting brown powder was recrystallized at 20 °C from either fluorobenzene (to yield **8a**) or THF/pentane (**8b**) as single crystals suitable for X-ray diffraction. Isolated yields 81% (for **8a**), 85% (for **8b**). Data for **8a**: ^{1}H NMR ($C_6D_5CD_3$, 300 MHz, 20 °C): δ 1.64, (s, 24H, *o*-CH_3 of IMes), 2.26 (s, 12H, *p*-CH_3 of IMes), 5.96, (s, 4H, NCHCHN of IMes), 6.75 (s, 8H, aromatic CH of IMes), 7.72 (s, 4H, *p*-CH of $[BAr^f_4]^-$), 8.35 (s, 8H, *o*-CH of $[BAr^f_4]^-$). ^{13}C NMR ($C_6D_5CD_3$, 126 MHz, 20 °C) (i) signals due to cation: δ 17.6 (*o*-CH_3 of IMes), 22.5 (*p*-CH_3 of IMes), 122.7 (NCHCHN of IMes), 129.7, (*o*-quaternary C of IMes), 135.8, (*m*-CH of IMes), 139.3 (*p*-quaternary C of IMes), 172.3 (br, carbene quaternary C of IMes), N-bound aryl quaternary signals not observed; (ii) signals due to anion: 118.0 (s, *p*-CH), 125.4 (q, J = 273.0 Hz, CF_3), 129.3 (q, J = 30.1 Hz, *m*-quaternary C), 134.7 (s, *o*-CH of anion), 162.3 (q, J = 49.1 Hz, *ipso*-quaternary C). ^{11}B NMR ($C_6D_5CD_3$, 96 MHz, 20 °C): δ −6.1. ^{19}F NMR ($C_6D_5CD_3$, 282 MHz, 20 °C): δ −62.5. IR (cm^{-1}): 1987 br [ν(N≡N)]. Anal. Calcd for $C_{74}H_{60}N_8BF_{24}Ir$: C, 51.64; H, 3.52; N, 6.51. Found: C, 51.47; H, 3.37; N, 6.23.

Data for 8b. ^{1}H NMR ($C_6D_5CD_3$, 300 MHz, 20 °C): δ 1.52 (m, 4H, THF), 1.72 (s, 24H, *o*-CH_3 of IMes), 2.19 (s, 12H, *p*-CH_3 of IMes), 3.39 (m, 4H, THF), 6.01 (s, 8H, NCHCHN of IMes), 6.70 (s, 4H, aromatic CH of IMes), 7.67 (s, 4H, *p*-CH of $[BAr^f_4]^-$), 8.32 (s, 8H, *o*-CH of $[BAr^f_4]^-$). ^{13}C NMR ($C_6D_5CD_3$, 126 MHz, 20 °C) (i) signals due to cation: δ 17.6 (s, *o*-CH_3 of IMes), 23.9 (*para*-CH_3 of IMes), 25.5, 68.1 (s, CH_2 of THF), 123.1 (NCHCHN of IMes), 129.7 (*o*-quaternary C of IMes), 135.5 (*m*-CH of IMes), 139.6 (*p*-quaternary C of IMes), 178.2 (carbene quaternary C of IMes). (ii) signals due to anion: 118.0 (s, *p*-CH), 127.3 (q, J = 273.0 Hz, CF_3), 129.9 (q, J = 30.1 Hz, *m*-quaternary C), 134.7 (s, *o*-CH), 162.8 (q, J = 49.2 Hz, *ipso*-quaternary C). ^{11}B NMR ($C_6D_5CD_3$, 96 MHz, 20 °C): δ −6.0. ^{19}F NMR ($C_6D_5CD_3$, 282 MHz, 20 °C): δ −58.0. IR (cm^{-1}): 1985 [ν(N≡N)]. Anal. Calcd for $C_{78}H_{68}N_6BF_{24}IrO$: C, 53.07; H, 3.89; N, 4.76. Found: C, 52.98; H, 3.65; N, 4.68.

$[M(IMes)_2(H)_2(\mu\text{-}H)_2B(H)\cdot NMe_3]^+[BAr^f_4]^-$ (M = Rh, 9; M = Ir, 10). Compounds **9** and **10** were prepared by a common method, illustrated here for compound **10**. To a suspension of **7** (0.43 g, 0.25 mmol) in fluorobenzene (50 cm^3) at −30 °C was added excess $Me_3N\cdot BH_3$ (0.37 g, 5.0 mmol), and the reaction mixture was warmed to 20 °C over a period of 1 h. After stirring for a further 6 h at 20 °C, the resulting pale yellow solution was filtered and concentrated in vacuo, and very pale yellow crystals suitable for X-ray diffraction were obtained by layering with pentane and storage at 20 °C. Isolated yield 0.33 g, 75%. ^{1}H NMR ($C_6D_5CD_3$, 300 MHz, 20 °C): δ −21.80 (s, 2H, IrH), −2.28 (br, 3H, BH_3), 1.53 (s, 9H, CH_3 of NMe_3), 1.63 (s, 24H, *o*-CH_3 of IMes), 2.26 (s, 12H, *p*-CH_3 of IMes), 6.04 (s, 4H, NCHCHN of IMes), 6.69 (s, 8H, aromatic CH of IMes), 7.71 (s, 4H, *p*-CH of $[BAr^f_4]^-$), 8.32 (s, 8H, *o*-CH of $[BAr^f_4]^-$). ^{13}C NMR ($C_6D_5CD_3$, 75 MHz, 20 °C) (i) signals due to cation: δ 18.3 (*o*-CH_3 of IMes), 51.1 (CH_3 of NMe_3), 121.7 (NCHCHN of IMes), 134.7 (*o*-quaternary C of IMes), 136.9 (*m*-CH of IMes), 138.2 (*p*-quaternary C of IMes), 170.3 (br, carbene quaternary C of IMes), *p*-CH_3 of IMes obscured by toluene solvent and N-bound aryl quaternary signals not observed; (ii) signals due to anion: 117.6 (s, *p*-CH), 124.9 (q, J = 272.9 Hz, CF_3), 129.5 (q, J = 31.7 Hz, *m*-quaternary C), 135.5 (s, *o*-CH), 162.3 (q, J = 50.3 Hz, *ipso*-quaternary C). ^{11}B NMR ($C_6D_5CD_3$, 96 MHz, 20 °C): δ −6.1 ($[BAr^f_4]^-$), 14.4 (br, $Me_3N\cdot BH_3$). ^{19}F NMR ($C_6D_5CD_3$, 282 MHz, 20 °C): δ −62.1. IR (cm^{-1}): 2497, 2272, 2001 [ν(B−H)]. Anal. Calcd for $C_{77}H_{74}N_5B_2F_{24}Ir$: C, 53.14; H, 4.29 N, 4.03. Found: C, 53.08; H, 4.32; N, 4.12.

Data for 9. Isolated yield 0.28 g, 68%. ^{1}H NMR ($C_6D_5CD_3$, 300 MHz, 20 °C): δ −18.77 (d, 2H, J = 27.0 Hz, RhH), −1.27 (br, 3H, BH_3), 1.56 (s, 9H, CH_3 of NMe_3), 1.62 (s, 24H, *o*-CH_3 of IMes), 2.25 (s, 12H, *p*-CH_3 of IMes), 6.03 (s, 4H, NCHCHN of IMes), 6.69 (s, 8H, aromatic CH of IMes), 7.70 (s, 4H, *p*-CH of $[BAr^f_4]^-$), 8.32 (s, 8H, *o*-CH of $[BAr^f_4]^-$). ^{13}C NMR ($C_6D_5CD_3$, 75 MHz, 20 °C) (i) signals due to cation: δ 18.4 (*o*-CH_3 of IMes), 22.0 (*p*-CH_3 of IMes), 52.4 (CH_3 of NMe_3), 122.5 (NCHCHN of IMes), 135.0, (*o*-quaternary C of IMes), 137.0 (*m*-CH of IMes), 138.7 (*p*-quaternary C of IMes), 184.3, (d, J = 41.5 Hz, carbene quaternary C of IMes), N-bound aryl quaternary signals not observed; (ii) signals due to anion: 118.1 (s, *p*-CH), 125.3 (1 q, J = 273.0 Hz, CF_3), 129.9 (q, J = 30.2 Hz, *m*-quaternary C), 135.5 (s, *o*-CH), 162.7 (q, J = 49.8 Hz, *ipso*-quaternary C). ^{11}B NMR ($C_6D_5CD_3$, 96 MHz, 20 °C): δ −6.0 (BAr^f anion), 1.5 (br, $Me_3N\cdot BH_3$). ^{19}F NMR ($C_6D_5CD_3$, 282 MHz, 20 °C): δ −62.2. IR (cm^{-1}): 2475, 2175, 1998 [ν(B−H)]. Anal. Calcd for $C_{77}H_{74}N_5B_2F_{24}Rh$): C, 56.02; H, 4.52 N, 4.24. Found: C, 55.90; H, 4.44; N, 4.18.

$[Rh(IMes)_2(H)_2(\mu\text{-}H)_2BNR_2]^+[BAr^f_4]^-$ (R = ^{i}Pr, 11; R = Cy, 12) and $[Ir(IMes)_2(H)_2(\mu\text{-}H)_2BNR_2]^+[BAr^f_4]^-$ (R = ^{i}Pr, 13; R = Cy, 14). Compounds **11**−**14** were prepared from **6** or **7** by a common method, illustrated here for compound **13**. To a suspension of **7**

(0.43 g, 0.25 mmol) in fluorobenzene (50 cm^3) at −30 °C was added excess $^iPr_2HN{\cdot}BH_3$ (0.57 g, 5.0 mmol), and the reaction mixture was warmed to 20 °C over a period of 1 h. After stirring for a further 6 h at 20 °C, the resulting deep brown solution was filtered and concentrated in vacuo, and yellow crystals of **13** suitable for X-ray diffraction were obtained by layering with pentane and storage at 20 °C. Isolated yield: 0.25 g, 56%. ^1H NMR ($C_6D_5CD_3$, 300 MHz, 20 °C): δ −15.50 (br, 2H, IrH), −5.83 (br, 2H, BH_2), 0.75 (d, J = 7.2 Hz, 12H, CH_3 of ^iPr), 1.51 (s, 24H, *o*-CH_3 of IMes), 2.24 (s, 12H, *p*-CH_3 of IMes), 2.79 (sept, J = 7.2 Hz, 2H, CH of ^iPr), 6.95 (s, 4H, NCHCHN of IMes), 6.65 (s, 8H, aromatic CH of IMes), 7.71 (s, 4H, *p*-CH of $[BAr^f_4]^-$), 8.33 (s, 8H, *o*-CH of $[BAr^f_4]^-$). ^{13}C NMR ($C_6D_5CD_3$, 75 MHz, 20 °C) (i) signals due to cation: 14.3 (CH_3 of ^iPr), 17.8 (*o*-CH_3 of IMes), 23.4 (*p*-CH_3 of IMes), 49.0 (CH of ^iPr), 122.1 (NCHCHN of IMes), 127.0 (*o*-quaternary C of IMes), 135.2 (*m*-CH of IMes), 138.7 (*p*-quaternary C of IMes), 172.9 (br, carbene quaternary C of IMes) N-bound aryl quaternary signal not observed; (ii) signals due to $[BAr^f_4]^-$ anion: 117.6 (s, *p*-CH), 123.1 (q, J = 273.0 Hz, CF_3), 129.6 (q, J = 32.7 Hz, *m*-quaternary C), 134.3 (s, *o*-CH), 162.6 (q, J = 50.3 Hz, *ipso*-quaternary C). ^{11}B NMR ($C_6D_5CD_3$, 96 MHz, 20 °C): δ −6.0 ($[BAr^f_4]^-$), 37.9 (br, $H_2B^iPr_2$). ^{19}F NMR ($C_6D_5CD_3$, 282 MHz, 20 °C): δ −62.1. IR (cm^{-1}): 2239 br [ν(B−H)]. Anal. Calcd for $C_{80}H_{78}N_5B_2F_{24}Ir$: C, 54.00; H, 4.42; N, 3.94. Found: C, 53.88; H, 4.33; N, 4.02.

Data for 11. Isolated yield 0.27 g, 68%. ^1H NMR (CD_2Cl_2, 300 MHz, 20 °C): δ −16.02 (br d, 2H, RhH), −1.40 (br, 2H, BH), 1.00 (d, J = 6.6 Hz, 6H, CH_3 of ^iPr), 1.01 (d, J = 6.6 Hz, 6H, CH_3 of ^iPr), 1.73 (s, 24H, *o*-CH_3 of IMes), 2.42(s, 12H, *p*-CH_3 of IMes), 3.14 (sept, J = 6.6 Hz, 2H, CH of ^iPr), 6.90 (s, 8H, *meta*-CH of IMes), 6.93 (s, 4H, NCH of IMes), 7.56 (s, 4H, *p*-CH of $[BAr^f_4]^-$), 7.73 (s, 8H, *o*-CH of $[BAr^f_4]^-$). ^{13}C NMR (CD_2Cl_2, 76 MHz, 20 °C) (i) signals due to cation: δ 15.8 (CH_3 of ^iPr), 18.8 (*o*-CH_3 of IMes), 22.1 (para-CH_3 of IMes), 49.3 (CH of ^iPr), 121.9 (NCH of IMes), 127.1 (*o*-quaternary C of IMes), 132.7 (*meta*-CH of IMes), 136.9 (*p*-quaternary C of IMes), 175.2 (br, carbene quaternary of IMes), N-bound aryl quaternary signals not observed; (ii) signals due to $[BAr^f_4]^-$ anion: 115.4 (s, *p*-CH), 123.9 (q, J = 272.1 Hz, CF_3), 127.1 (q, J = 32.3 Hz, *m*-quaternary C), 134.3 (*o*-CH), 159.7 (q, J = 49.8 Hz, *ipso*-quaternary C). ^{11}B NMR (CD_2Cl_2, 96 MHz, 20 °C): δ −6.0 ($[BAr^f_4]^-$), 35.4 (br, $H_2B^iPr_2$). ^{19}F NMR (CD_2Cl_2, 282 MHz, 20 °C): δ −62.1. IR (cm^{-1}): 2049 br [ν(B−H)]. Anal. Calcd for $C_{80}H_{78}N_5B_2F_{24}Rh$: C, 56.86; H, 4.65 N, 4.14. Found: C, 56.74; H, 4.54; N, 4.09.

Data for 12. Isolated yield 0.31 g, 71%. ^1H NMR ($C_6D_5CD_3$, 300 MHz, 20 °C): δ −15.90 (br d, J = ca. 25 Hz, 2H, RhH), −1.74 (br, 2H, BH_2), 0.88 to 2.51 (overlapping m, 22H, CH_2 of Cy), 1.51 (s, 24H, *o*-CH_3 of IMes), 2.24 (s, 12H, *p*-CH_3 of IMes), 2.50 (m, 2H, CH of Cy), 5.96 (s, 4H, NCHCHN of IMes), 6.64 (s, 8H, aromatic CH of IMes), 7.69 (s, 4H, *p*-CH of $[BAr^f_4]^-$), 8.33 (s, 8H, *o*-CH of $[BAr^f_4]^-$). ^{13}C NMR ($C_6D_5CD_3$, 126 MHz, 20 °C) (i) signals due to cation: δ 17.6 (*o*-CH_3 of IMes), 22.8 (*p*-CH_3 of IMes), 25.3, 25.5, 26.2, 26.8, 34.9 35.2 (CH_2 of Cy), 53.3, 60.6 (CH of Cy) 122.0 (NCHCHN of IMes), 129.5 (*o*-quaternary C of IMes) 135.5 (*meta*-CH of IMes), 139.1 (*p*-quaternary C of IMes),176.5 (br, carbene quaternary C of IMes), N-bound aryl quaternary signals not observed; (ii) signals due to $[BAr^f_4{}^-]$ anion: 117.9 (s, *p*-CH), 125.8 (q, J = 272.9 Hz, CF_3), 130.1 (q, J = 30.3 Hz, *m*-quaternary C), 134.7 (s, *o*-CH), 162.6 (q, J = 49.6 Hz, *ipso*-quaternary C). ^{11}B NMR ($C_6D_5CD_3$, 96 MHz, 20 °C): δ −6.0 ($BAr^f_4]^-$), 35.8 (br, H_2BNCy_2). ^{19}F NMR ($C_6D_5CD_3$, 282 MHz, 20 °C): δ −62.2. IR (cm^{-1}): 2040 br [ν(B−H)]. Anal. Calcd for $C_{86}H_{86}N_5B_2F_{24}Rh$: C, 58.35; H, 4.90 N, 3.98. Found: C, 58.28; H, 4.85; N, 3.90.

Data for 14. Isolated yield 0.32 g, 69%. ^1H NMR ($C_6D_5CD_3$, 300 MHz, 20 °C): δ −15.44 (br s, 2H, IrH), −5.83 (br s, 2H, BH_2), 0.87 to 2.64 (overlapping m, 22H, CH_2 of Cy), 1.52 (s, 24H, *o*-CH_3 of IMes), 2.17(s, 12H, *p*-CH_3 of IMes), 2.48 (overlapping m, 2H, CH of Cy), 5.96 (s, 4H, NCHCHN of IMes), 6.65 (s, 8H, aromatic CH of IMes), 7.70 (s, 4H, *p*-CH of $[BAr^f_4]^-$), 8.32 (s, 8H, *o*-CH of $[BAr^f_4]^-$). ^{13}C NMR ($C_6D_5CD_3$, 75 MHz, 20 °C) (i) signals due to cation: δ 17.8 (*o*-CH_3 of IMes), 23.3 (*p*-CH_3 of IMes), 23.5, 24.8, 25.9, 29.4, 29.6, 34.5 (CH_2 of Cy), 55.8, 58.2 (CH of Cy) 122.1 (NCHCHN of IMes), 129.1 (*o*-quaternary C of IMes) 134.4 (*meta*-CH of IMes), 138.6 (*p*-quaternary C of IMes), carbene quaternary C of IMes and N-bound aryl quaternary signals not observed; (ii) signals due to anion: 117.6 (s, *p*-CH), 124.9 (q, J = 273.0 Hz, CF_3), 129.4 (q, J = 31.7 Hz, *m*-quaternary C), 135.1 (s, *o*-CH), 162.2 (q, J = 50.3 Hz, *ipso*-quaternary C). ^{11}B NMR ($C_6D_5CD_3$, 96 MHz, 20 °C): δ −6.1 ($BAr^f_4]^-$), 35.9 (br, H_2BNCy_2). ^{19}F NMR ($C_6D_5CD_3$, 282 MHz, 20 °C): δ −61.2. IR (cm^{-1}): 2236 br [ν(B−H)]. Anal. Calcd for $C_{86}H_{86}N_5B_2F_{24}Ir$: C, 55.52; H, 4.66, N, 3.77. Found: C, 55.24; H, 4.32; N, 3.66.

$[Rh(IMes)_2(H)_2(\mu\text{-}H)_2B(H){\cdot}NH_2{}^tBu]^+[BAr^f_4]^-$ (15). To a suspension of **6** (0.41 g, 0.25 mmol) in fluorobenzene (50 cm^3) at −30 °C was added excess $^tBuH_2N{\cdot}BH_3$ (0.44 g, 5 mmol), and the reaction mixture was warmed to 20 °C over a period of 1 h. After stirring for a further 6 h, the resulting deep brown solution was filtered and concentrated in vacuo, and very pale yellow crystals of **15** suitable for X-ray diffraction were obtained by layering with pentane and storage at 20 °C. Isolated yield: 0.21 g, 51%. ^1H NMR ($C_6D_5CD_3$, 300 MHz, 20 °C): δ −17.95 (d, 2H, J = 29.7 Hz, RhH), −1.66 (br, 3H, BH_3), 0.49 (s, 9H, CH_3 of ^tBu), 0.26, 0.43, 1.37, 2.07 (s, each 3H, *p*-CH_3 of IMes), 1.58 (2 overlapping signals), 1.72, 2.14 (s, each 6H, ortho-CH_3 of IMes), 5.76, 5.98 (s, each 2H, NCHCHN of IMes), 6.65, 6.67 (s, each 4H, aromatic CH of IMes), 7.65(s, 4H, *p*-CH of $[BAr^f_4]^-$), 8.35(s, 8H, *o*-CH of $[BAr^f_4]^-$). ^{13}C NMR ($C_6D_5CD_3$, 126 MHz, 20 °C) (i) signals due to cation: δ 14.4 (CH_3 of ^tBu), 17.1, 18.1, 21.0, 21.1, 22.8, 27.2 (2 overlapping signals), 34.1 (CH_3 of IMes), 55.3 (quaternary C of ^tBu), 121.0, 122.7 (NCHCHN of IMes), 127.8, 129.3 (*o*-quaternary C of IMes), 135.4 (2 overlapping signals, *m*-CH of IMes), 139.1, 140.2 (*p*-quaternary C of IMes), carbene quaternary of IMes and N-bound aryl quaternary signal not observed; (ii) signals due to $[BAr^f_4]^-$ anion: 118.1 (s, *p*-CH), 125.3 (q, J = 271.9 Hz, CF_3), 129.7 (q, J = 29.6 Hz, *m*-quaternary C), 134.6 (s, *o*-CH), 162.7 (q, J = 50.2 Hz, *ipso*-quaternary C). ^{11}B NMR ($C_6D_5CD_3$, 96 MHz, 20 °C): δ −6.2 ($[BAr^f_4]^-$), −35.1 (q, J = 83.1 Hz, $H_3B{\cdot}NH_2{}^tBu$). ^{19}F NMR ($C_6D_5CD_3$, 282 MHz, 20 °C): δ −61.3. IR (cm^{-1}): 2501, 1996, 1961 [ν(B−H)]. Anal. Calcd for $C_{78}H_{68}N_5B_2F_{24}Rh$: C, 56.29; H, 4.06 N, 4.23. Found: C, 56.21; H, 4.13; N, 4.17.

$[Rh(IMes)_2(H)_2(\mu\text{-}H)_2BNH{}^tBu]^+[BAr^f_4]^-$ (16). Prepared from **6** and a 20-fold excess of $^tBuH_2N{\cdot}BH_3$ in a similar manner to **15**, with the exception that the reaction mixture was left to stir for a total of 48 h at 20 °C. The resulting fluorobenzene solution was filtered, concentrated in vacuo, and intense yellow crystals suitable for X-ray diffraction were obtained by layering with pentane and storage at 20 °C. Isolated yield 0.32 g, 72%. ^1H NMR ($C_6D_5CD_3$, 300 MHz, 20 °C): δ −21.69 (d, J = 51 Hz, 2H RhH), −2.62 (br, 2H, BH_2), 0.52 (s, 9H, CH_3 of ^tBu), 1.63 (s, 24H, *o*-CH_3 of IMes), 2.22 (s, 12 H, *p*-CH_3 of IMes), 5.97 (s, 4H, NCHCHN of IMes), 6.58 (s, 8H, aromatic CH of IMes), 7.70 (s, 4H, *p*-CH of $[BAr^f_4]^-$), 8,34 (s, 8H, *o*-CH of $[BAr^f_4]^-$). ^{13}C NMR ($C_6D_5CD_3$, 126 MHz, 20 °C) (i) signals due to cation: δ 18.5 (*o*-CH_3 of IMes), 23.2 (*p*-CH_3 of IMes), 31.0 (CH_3 of ^tBu), 56.4 (quaternary C of ^tBu), 122.4, (NCHCHN of IMes), 129.4 (*o*-quaternary C of IMes), 135.0 (*m*-CH of IMes), 139.5 (*p*-quaternary C of IMes), carbene quaternary of IMes and N-bound aryl quaternary signal not observed; (ii) signals due to $[BAr^f_4]^-$ anion: 118.4 (s, *p*-CH), 125.6 (q, J = 273.0 Hz, CF_3), 130.3 (q, J = 33.9 Hz, *m*-quaternary C), 135.9 (s, *o*-CH), 163.0 (q, J = 50.3 Hz, *ipso*-quaternary C). ^{11}B NMR ($C_6D_5CD_3$, 96 MHz, 20 °C): δ −6.1 ($[BAr^f_4]^-$), 37.4 (br, $H_2BNH{}^tBu$). ^{19}F NMR ($C_6D_5CD_3$, 282 MHz, 20 °C): δ −61.9. IR (cm^{-1}): 2171 [ν(B−H)]. Anal. Calcd for $C_{78}H_{74}N_5B_2F_{24}Rh$: C, 56.34; H, 4.49 N, 4.21. Found: C, 56.43; H, 4.38; N, 4.23.

$[Ir(IMes)(IMes')(H)(\mu\text{-}H)_2BNCy_2]^+[BAr^f_4]^-$ (17). To a suspension of **7** (0.43 g, 0.25 mmol) in fluorobenzene (50 cm^3) at −30 °C was added excess $Cy_2HN{\cdot}BH_3$ (0.98 g, 5 mmol), and the reaction mixture was warmed to 20 °C over a period of 1 h. After

stirring for a further 6 h at 20 °C, 3,3-dimethylbutene (TBE; ca. 10 equiv) was added, and the reaction was allowed to continue for a further 6 h. The resulting light brown solution was filtered and concentrated in vacuo, and yellow crystals suitable for X-ray diffraction were obtained by layering with pentane and storage at 20 °C. Isolated yield 0.29 g, 63%. ^{1}H NMR ($C_6D_5CD_3$, 300 MHz, 20 °C): δ −15.43 (s, 1H, IrH), −10.88 (br s, 1H, BH), −5.81 (br s, 1H, BH), 0.85 to 2.50 (overlapping m, 20H, CH_2 of Cy), 1.51 (s, 12H, *o*-CH_3 of IMes), 1.61, 1.71, 1.85 (s, each 3H, *o*-CH_3 of IMes′), 1.92 (br, 2H, CH_2Ir), 2.09, 2.14 (s, each 3H, *p*-CH_3 of IMes′), 2.24 (s, 6H, *p*-CH_3 of IMes), 2.46 (overlapping m, 2H, CH of Cy), 5.96 (s, 2H, NCHCHN of IMes), 6.01, 6.07 (br s, each 1H, NCHCHN of IMes′), 6.56 (s, 2H, aromatic CH of IMes′), 6.65 (s, 4H, aromatic CH of IMes), 6.69, 6.75 (s, each 1H, aromatic CH of IMes′), 7.70 (s, 4H, *p*-CH of $[BAr^f_4]^-$), 8.32 (s, 8H, *o*-CH of $[BAr^f_4]^-$). ^{13}C NMR ($C_6D_5CD_3$, 75 MHz, 20 °C) (i) signals due to cation: δ 17.3, 17.8, 17.9, 18.1 (*o*-CH_3 of IMes and IMes′), 24.5, 24.8, 25.2 (*p*-CH_3 of IMes and IMes′), 25.3, 25.9, 32.0, 32.8, 33.5 34.5, (CH_2 of Cy), 53.6 (CH_2Ir), 55.3, 58.2 (CH of Cy), 121.0, 122.0, 122.6 (NCHCHN of IMes and IMes′), 129.7, 130.3, 130.5, 131.4, 131.6 (*o*-quaternary C of IMes and IMes′), 134.4, 134.5, 135.2, 135.4, 136.6 (*m*-CH of IMes and IMes′), 138.6, 139.2, 140.1 (*p*-C of IMes and IMes′), carbene quaternary of IMes/IMes′ and N-bound aryl quaternary signals not observed; (ii) signals due to anion: 117.5 (s, *p*-CH), 124.9 (q, J = 273.0 Hz, CF_3), 129.9 (q, J = 30.2 Hz, *m*-quaternary C), 135.1 (s, *o*-CH), 162.3 (q, J = 48.3 Hz, *ipso*-quaternary C). ^{11}B NMR ($C_6D_5CD_3$, 96 MHz, 20 °C): δ −6.0 ($[BAr^f_4]^-$), 36.2 (br, H_2BNCy_2). ^{19}F NMR ($C_6D_5CD_3$, 282 MHz, 20 °C): δ −61.2. IR (cm^{-1}): 2256 [ν(B−H)]. Anal. Calcd for $C_{86}H_{84}N_5B_2F_{24}Ir$: C, 55.58; H, 4.56, N, 3.77. Found: C, 55.50; H, 4.45; N, 3.64.

$[Ir(IMes)(IMes′)(H)BNCy_2]^+[BAr^f_4]^-$ (18). A suspension of **17** (0.19 g, 0.10 mmol) in toluene (50 cm^3) was heated at 65 °C with vigorous stirring for a period of 36 h. The reaction mixture was concentrated and layered with pentane, yielding **18** as bright yellow crystals suitable for X-ray diffraction. Isolated yield 0.15 g, 82%. ^{1}H NMR ($C_6D_5CD_3$, 300 MHz, 20 °C): δ −10.85 (s, fwhm 43 Hz, fwhm ^{1}H{^{11}B} 12 Hz, 1H, IrHB), 0.45 to 1.80 (overlapping m, 20H, CH_2 of Cy), 1.16, 1.88 (s, each 3H, *o*-CH_3 of IMes′), 2.00, 2.09 (s, each 6H, *o*-CH_3 of IMes), 2.28 (s, 3H, *o*-CH_3 of IMes′), 1.75 (d J = 12 Hz, 1H, CH_2Ir), 2.34 (s, 3H, *p*-CH_3 of IMes′), 2.36 (s, 6H, *p*-CH_3 of IMes), 2.39 (s, 3H, *p*-CH_3 of IMes′), 2.39 (d J = 12 Hz, 1H, CH_2Ir), 2.50 (overlapping m, 2H, CH of Cy), 6.81, 6.84 (br s, each 1H, NCHCHN of IMes′), 6.91 (br s, 4H, aromatic CH of IMes), 7.00 (br s, 2H, aromatic CH of IMes′), 7.03 (s, 2H, NCHCHN of IMes), 7.06 (d J = 2 Hz, 1H, aromatic CH of IMes′), 7.61 (d J = 2 Hz, 1H, aromatic CH of IMes′), 7.58 (s, 4H, *p*-CH of $[BAr^f_4]^-$), 7.74 (s, 8H, *o*-CH of $[BAr^f_4]^-$). ^{13}C NMR (CD_2Cl_2, 75 MHz, 20 °C) (i) signals due to cation: δ 17.3, 17.6, 18.0, 18.4, 18.9 (*o*-CH_3 of IMes and IMes′), 20.7, 21.1, 21.7 (*p*-CH_3 of IMes and IMes′), 25.0, 25.3, 30.4, 30.6, 32.3, 33.4, (CH_2 of Cy), 34.2 (CH_2Ir), 55.3, 58.2 (CH of Cy), 116.9, 117.7, 118.0 (NCHCHN of IMes and IMes′), 128.7, 129.3, 129.8, 130.1, 130.4 (*o*-quaternary C of IMes and IMes′), 134.4, 134,7, 134.8, 135.2, 135.5 (*m*-CH of IMes and IMes′), 139.3, 139.3, 140.9 (*p*-C of IMes and IMes′), 174.4, 177.2 (carbene quaternary C of IMes and IMes′), N-bound aryl quaternary signals not observed; (ii) signals due to anion: 117.1 (s, *p*-CH), 124.6 (q, J = 272.0 Hz, CF_3), 128.9 (q, J = 32.2 Hz, *m*-quaternary C), 135.0 (s, *o*-CH), 162.3 (q, J = 46.0 Hz, *ipso*-quaternary C). ^{11}B NMR (CD_2Cl_2, 96 MHz, 20 °C): δ −6.0 ($[BAr^f_4]^-$), 38.0 (br, $HBNCy_2$). ^{19}F NMR ($C_6D_5CD_3$, 282 MHz, 20 °C): δ −62.8. IR (cm^{-1}): 2254 [ν(B−H)]. Anal. Calcd for $C_{86}H_{82}N_5B_2F_{24}Ir$: C, 55.64; H, 4.46, N, 3.77. Found: C, 55.50; H, 4.45; N, 3.64.

Crystal Structure Determination. Data for **4**, **8a**, **8b**, **9**, **10**, **14**, **16**, **17**, **18** and $[(IMes)BH_2NH_3]^+[BAr^f_4]^-$ were collected on a Nonius KappaCCD diffractometer (Mo Kα radiation; λ = 0.71073 Å) with an Oxford Cryosystems N_2 open-flow cooling device.[26a] Unit cell parameters and intensity data were processed using the DENZO-SMN package, and reflection intensities were corrected for absorption effects by the multiscan method, based on multiple scans of identical and Laue equivalent reflections.[26b] Data for $[Rh(IMes)_2(H)_2(THF)]^+[BAr^f_4]^-$ were collected on Beamline I19 (EH1) at the Diamond Light Source, and raw frame data were processed using CrystalClear.[26c] All structures were solved using SIR92, and refinement was carried out using full-matrix least-squares within the CRYSTALS suite,[26d,e] on either F^2 or F (the latter for $[Rh(IMes)_2(H)_2(THF)]^+[BAr^f_4]^-$ only). In general, all non-hydrogen atoms were refined with anisotropic displacement parameters. The nature of the $[BAr^f_4]^-$ anion means that all structures exhibited disordered CF_3 groups, the most extreme examples of which were modeled using two rotationally offset components with distances and thermal parameters controlled using "same distance" and rigid bond restraints. In one or two cases, out of plane motion was also evident and the model was adjusted accordingly. For compound **8a** it was evident that one of the dinitrogen sites was partially occupied by other components and a 3-fold disordered model was used; similar disorder was observed in $[Rh(IMes)_2(H)_2(THF)]^+[BAr^f_4]^-$. Compounds **9**, **14**, and **16** also exhibit disorder in the amineborane ligand; in the cases of **9** and **16**, the orientational disorder affected the whole ligand, whereas in **14** only the cyclohexyl groups were affected. In each case the disorder was modeled appropriately and the components restrained to give similar geometry and thermal behavior.

In general, hydrogen atoms were visible in the difference map, but alkyl/aromatic hydrogen atoms were positioned geometrically, and their positions and isotropic displacement parameters were refined using restraints prior to inclusion into the model with riding constraints. Other hydrogen atoms were located by examination of the difference Fourier map. In cases where this was challenging, the contribution to the scattering from the hydrogen atoms was increased by truncating the data to ca. 1.1 Å, which had the effect of enhancing peaks due to the presence of hydrogen atoms. Once located in this way, hydrogen atoms were generally then treated as described above; exceptions to this procedure were in the case of the disordered components in compounds **8a**, **16**, and $[Rh(IMes)_2(H)_2(THF)]^+[BAr^f_4]^-$, where it was necessary to place some hydrogen atoms at sensible geometric positions. For riding hydrogen atoms, standard uncertainties were calculated from the final refinement using the full variance covariance matrix for distances where this was applicable.

All standard uncertainties were calculated using the full variance covariance matrix within CRYSTALS unless otherwise stated. After final convergence, dummy atoms were placed at the calculated centroid positions where required. Distances and standard uncertainties were then calculated after a single least-squares cycle with all atoms constrained to ride within CRYSTALS; in each case the maximum shift changed by less than 50% of the final refined value.

Selected structural details for the new compounds are included in Table 1, and full crystallographic data for all structures have been deposited with the Cambridge Crystallographic Data Centre, CCDC 777346−777356. Structural details for compounds **5**, **7**, **11**, **12**, **13**, and **15** were included in a preliminary communication of part of this work[17] and can be accessed from the CCDC using reference numbers 758029−758034. Copies of these data can be obtained free of charge from The Cambridge Crystallographic Data Centre via www.ccdc.cam.ac.uk/data_request/cif.

Results and Discussion

Halide abstraction is well established as a synthetic methodology for the generation of highly reactive cationic species stabilized, for example, by weak agostic or solvent molecule derived interactions.[16a,b] We have employed this synthetic approach in association with the strongly σ donating NHC class of ligand[18] to target systems of the type $[ML_2(H)_2]^+$. Thus, the reactions of $M(IPr)_2(H)_2Cl$ (**1**) and $M(IMes)_2(H)_2Cl$ (M = Rh, **2**; M = Ir, **3**) toward the potent halide abstraction agent

Table 1. Crystallographic Data for **4**, **8a**, **8b**, **9**, **10**, **14**·0.37(C_5H_{12}), **16**, **17**, and **18**

	4	**8a**	**8b**
CCDC deposition number	777346	777347	777348
empirical formula	$C_{86}H_{86}B_{24}IrN_4$	$C_{74}H_{60.43}BCl_{0.15}F_{24}N_{7.27}Na_{0.15}Ir$	$C_{78}H_{68}BF_{24}N_6OIr$
formula weight	1834.64	1719.28	1764.42
temperature (K)	150	150	150
wavelength (Å)	0.71073	0.71073	0.71073
crystal system	monoclinic	monoclinic	monoclinic
space group	$P2_1/c$	$P2/n$	$P2/n$
unit cell lengths: *a*, *b*, *c* (Å)	20.8509(1)	12.7677(1)	12.9101(1)
	17.1103(1)	14.3005(1)	14.4822(1)
	24.2437(2)	20.9203(2)	20.7483(2)
α, *β*, *γ* (deg)	90, 104.1813(2), 90	90, 95.129(1), 90	90, 95.7575(4), 90
volume (Å^3), Z	8385.72(9)	3804.43(5), 2	3859.67(5), 2
density (calcd) (Mg/m^3)	1.453	1.501	1.518
absorption coeff (mm^{-1})	1.692	1.866	1.836
F(000)	3712	1715	1768
crystal size (mm^3)	0.06 × 0.21 × 0.23	0.11 × 0.16 × 0.21	0.08 × 0.15 × 0.18
θ range for data collectn (deg)	5.100 to 27.493	5.19 to 27.49	5.14 to 27.41
index ranges (*h*, *k*, *l*)	−27 to 27, −22 to 22, −31 to 31	16, 18, 27	−16 to 16, −18 to 18, −26 to 26
no. of reflections collected	139522	60119	71076
no. of indep reflns/R_{int}	19077 (0.045)	8668 (0.031)	8701 (0.020)
completeness to θ_{max} (%)	0.990	99.2	99.0
absorption correction	multiscan	multiscan	multiscan
max and min transmission	0.77 and 0.90	0.81, 0.75	0.86, 0.80
refinement method	full matrix least-squares on F^2	full matrix least-squares on F^2	full matrix least-squares on F^2
no. data/restraints/params	19077/648/1157	8668/334/553	8700/324/560
goodness-of-fit on F^2	0.9577	0.9531	1.0001
final *R* indices [$I > 2\sigma(I)$]	$R1 = 0.0412$, $wR2 = 0.0813$	$R1 = 0.0481$, $wR2 = 0.1009$	$R1 = 0.0375$, $wR2 = 0.0894$
R indices (all data)	$R1 = 0.0674$, $wR2 = 0.1007$	$R1 = 0.0621$, $wR2 = 0.1165$	$R1 = 0.0431$, $wR2 = 0.0961$
largest peak/hole (e Å^{-3})	2.59, −1.12	1.09, −3.36	1.99, −0.97

	9	**10**	**14**·0.37(C_5H_{12})
CCDC deposition number	777349	777350	777351
empirical formula	$C_{77}H_{74}B_2F_{24}N_5Rh$	$C_{77}H_{74}B_2F_{24}IrN_5$	$C_{87.84}H_{90.41}B_2F_{24}N_5Ir$
formula weight	1649.95	1739.26	1885.99
temperature (K)	150	150	150
wavelength (Å)	0.71073	0.71073	0.71073
crystal system	triclinic	triclinic	triclinic
space group	*P*-1	*P*-1	*P*-1
unit cell lengths: *a*, *b*, *c* (Å)	12.3626(1)	12.5131(1)	13.0196(1)
	18.0479(1)	18.0250(2)	16.2636(1)
	18.2196(2)	18.3267(2)	41.958(3)
α, *β*, *γ* (deg)	85.750(1), 89.665(1), 73.417(1)	92.264(1), 109.900(1), 92.529(4)	86.177(1), 89.955(1), 84.565(1)
volume (Å^3), Z	3884.84(6), 2	3876.41(7), 2	8824.6(6), 4
density (calcd) (Mg/m^3)	1.410	1.490	1.419
absorption coeff (mm^{-1})	0.323	1.825	1.610
F(000)	1684	1748	3821.8
crystal size (mm^3)	0.14 × 0.18 × 0.20	0.11 × 0.16 × 0.18	0.11 × 0.16 × 0.25
θ range for data collectn (deg)	5.11 to 27.53	5.11 to 27.53	5.10 to 27.52
index ranges (*h*, *k*, *l*)	−16 to 16, −23 to 23, −23 to 23	−16 to 16, −22 to 23, −23 to 23	−16 to 16, −20 to 20, 0 to 54
no. of reflections collected	69814	63853	99224
no. of indep reflns/R_{int}	17698 (0.024)	17624 (0.029)	38802 (0.029)
completeness to θ_{max} (%)	98.9	98.6	95.6
absorption correction	multiscan	multiscan	multiscan
max and min transmission	0.96, 0.93	0.82, 0.74	0.84, 0.77
refinement method	full matrix least-squares on F^2	full matrix least-squares on F^2	full matrix least-squares on F^2
no. data/restraints/params	17697/552/1084	17624/324/1038	33463/1394/2421
goodness-of-fit on F^2	0.9992	0.9988	0.9993
final *R* indices [$I > 2\sigma(I)$]	$R1 = 0.0505$, $wR2 = 0.1192$	$R1 = 0.0393$, $wR2 = 0.0888$	$R1 = 0.0789$, $wR2 = 0.1520$
R indices (all data)	$R1 = 0.0624$, $wR2 = 0.1324$	$R1 = 0.0523$, $wR2 = 0.1030$	$R1 = 0.0963$, $wR2 = 0.1652$
largest peak/hole (e Å^{-3})	1.49, −1.19	2.06, −1.35	4.54, −5.65

	16	**17**	**18**
CCDC deposition number	777352	777353	777354
empirical formula	$C_{78}H_{74}B_2F_{24}N_5Rh$	$C_{86}H_{84}B_2F_{24}N_5Ir$	$C_{86}H_{82}B_2F_{24}N_5Ir$
formula weight	1661.96	1857.44	1855.42
temperature (K)	150	150	150
wavelength (Å)	0.71073	0.71073	0.71073
crystal system	triclinic	triclinic	monoclinic
space group	*P*-1	*P*-1	$P2_1/n$
unit cell lengths: *a*, *b*, *c* (Å)	12.5092(1)	12.9838(2)	13.4156(1)
	18.0131(2)	18.0619(2)	16.6035(2)
	18.2799(2)	19.1755(3)	38.5024(4)

Table 1. Continued

	16	17	18
α, *β*, *γ* (deg)	86.989(1), 70.691(1), 87.986(1)	89.919(1), 72.222(1), 85.174(1)	90, 95.1242(4), 90
volume (Å^3), Z	3881.23(7), 2	4265.57(11), 2	8541.98(15), 4
density (calcd) (Mg/m^3)	1.422	1.446	1.443
absorption coeff (mm^{-1})	0.324	1.664	1.662
F(000)	1696	1876	3744
crystal size (mm^3)	0.11 × 0.16 × 0.20	0.06 × 0.14 × 0.19	0.03 × 0.14 × 0.16
θ range for data collectn (deg)	5.11 to 27.50	5.11 to 27.54	5.12 to 27.49
index ranges (*h*, *k*, *l*)	−15 to 16, −22 to 23, −23 to 23	−16 to 16, −23 to 23, −24 to 24	−17 to 17, 0 to 21, 0 to 50
no. of reflections collected	49251	64780	20092
no. of indep reflns/R_{int}	17537 (0.036)	19371 (0.037)	19437 (0.064)
completeness to θ_{max} (%)	98.4	98.4	99.1
absorption correction	multiscan	multiscan	multiscan
max and min transmission	0.97 and 0.84	0.90 and 0.80	0.95 and 0.62
refinement method	full matrix least-squares on F^2	full matrix least-squares on F^2	full matrix least-squares on F^2
no. data/restraints/params	17537/1158/1177	19370/648/1175	19410/747/1194
goodness-of-fit on F^2	0.9995	0.9999	0.9531
final *R* indices [$I > 2\sigma(I)$]	$R1 = 0.0653$, $wR2 = 0.1604$	$R1 = 0.0582$, $wR2 = 0.1240$	$R1 = 0.0654$, $wR2 = 0.1085$
R indices (all data)	$R1 = 0.0820$, $wR2 = 0.1822$	$R1 = 0.0788$, $wR2 = 0.1405$	$R1 = 0.1103$, $wR2 = 0.1380$
largest peak/hole (e Å^{-3})	1.66, −1.23	1.80, −1.44	3.72, −3.25

Scheme 1. Isopropyl Group Dehydrogenation Initiated by Chloride Abstraction; Isolation of Bis(agostic) Intermediate **4**[a]

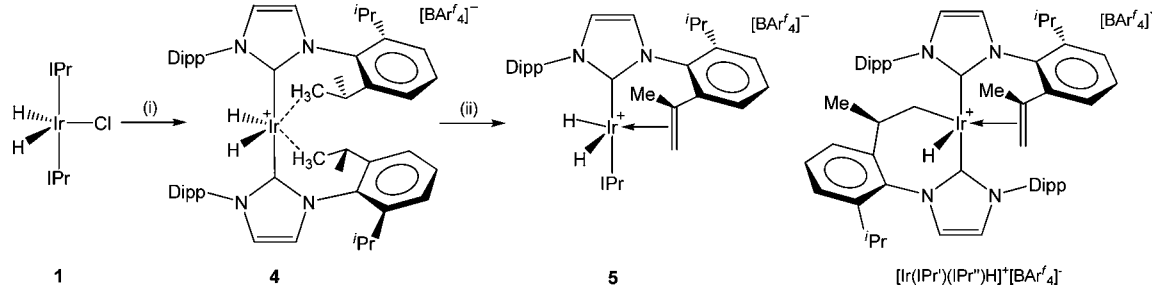

[a] Key reagents and conditions: (i) Na[BAr$^f_4$], fluorobenzene, 3 h at 20°C, 65%; (ii) from **1**: Na[BAr$^f_4$], fluorobenzene, 12 h at 20°C, 78%.

Na[BAr$^f_4$] [Ar^f = 3,5-C$_6$H$_3$(CF$_3$)$_2$] have been investigated; in the event such chemistry leads to the formation of highly reactive cationic species capable of the dehydrogenation of saturated CC and BN linkages.

IPr Systems. The reaction of Ir(IPr)$_2$(H)$_2$Cl (**1**) with Na[BAr$^f_4$] in fluorobenzene over 3 h generates [Ir(IPr)$_2$(H)$_2$]$^+$[BAr$^f_4$]$^-$ (**4**) in 65% isolated yield, with the iridium center stabilized by a pair of agostic interactions utilizing the methyl groups of the isopropyl substituents (Scheme 1). ^{1}H NMR data for **4** in toluene-d_8 solution show only two ^{i}Pr methyl resonances (even at 200 K), consistent with rapid fluxional exchange; the IR spectrum of **4** in solution, however, reveals a C−H stretching band at 2711 cm^{-1} in the region characteristic of C−H···Ir agostic systems.[16a] More definitive evidence for agostic stabilization of the metal center comes from crystallographic measurements in the solid state (Figure 1).

Geometrically, the structure of the cationic component of **4** features *trans* IPr [∠C(2)−Ir(1)−C(31) = 177.3(2)°], *cis* hydride and *cis* C−H agostic ligands (clearly visible in the difference Fourier map) and is thus reminiscent of bis(phosphine) and bis(NHC) iridium(III) complexes reported by Caulton and Nolan.[10b,c,16a,b] The Ir···C distances associated with the C−H agostic ligands in **4** [2.943(5) and 3.049(5) Å] are slightly longer than those reported for the bis(phosphine) system [Ir(PPh^{t}Bu$_2$)$_2$(H)$_2$]$^+$ (2.81−2.94 Å) and for the closely related rhodium complex [Rh(P^{i}Bu$_3$)$_2$(H)$_2$]$^+$ [2.90(3) and 2.891(5) Å];[16c] the corresponding distances reported for [Ir(I^{t}Bu)$_2$(H)$_2$]$^+$ (2.653 Å) are significantly shorter than any of these three systems.[10b,c]

After prolonged (12 h) reaction at 20 °C, C−H activation leads to the dehydrogenation of one of the carbene ^{i}Pr substituents and the formation of [Ir(IPr)(IPr″)(H)$_2$]$^+$[BAr$^f_4$]$^-$ (**5**), featuring the mixed NHC/alkene donor IPr″ ligand (Scheme 1). This type of isopropyl dehydrogenation chemistry has recently been observed for Ir(I) bis(NHC) systems and has wider precedent in the chemistry of phosphine, *β*-ketiminate, and other classes of donors featuring pendant substituents such as isopropyl, cyclohexyl or cyclopentyl.[11–14] Spectroscopically, isopropyl dehydrogenation is signaled by a significant increase in the complexity of the ^{i}Pr Me and CH signals and by the appearance of two alkene CH resonances and a singlet at δ_H 1.15 corresponding to the remaining unactivated methyl group of the -(Me)C=CH$_2$ moiety. While further characterization by

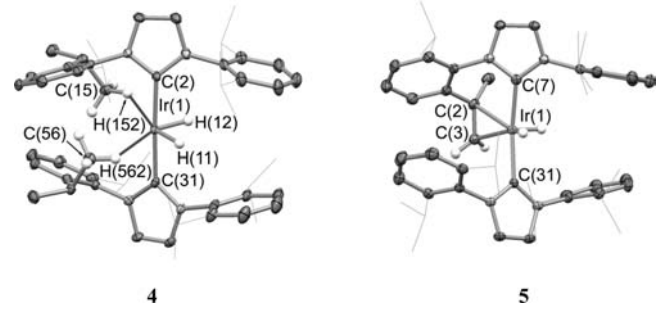

Figure 1. Molecular structures of the cationic components of **4** and **5**; hydrogen atoms [except those attached to Ir(1), C(15) and C(56) (for **4**), and Ir(1) and C(3) (for **5**)] omitted for clarity, and thermal ellipsoids set at the 40% probability level. Key distances (Å) and angles (deg): (for **4**) Ir(1)···C(15) 3.049(5), Ir(1)···C(56) 2.943(5), Ir(1)−H(152) 2.207(5), Ir(1)−C(562) 2.117(5); (for **5**) Ir(1)−C(2) 2.275(3), Ir(1)−C(3) 2.239(4), C(7)−Ir(1)−C(31) 162.64(3).

Scheme 2. Synthesis of NaCl Inclusion Compounds **6** and **7** and Subsequent Reactivity of **7** with Dinitrogen[a]

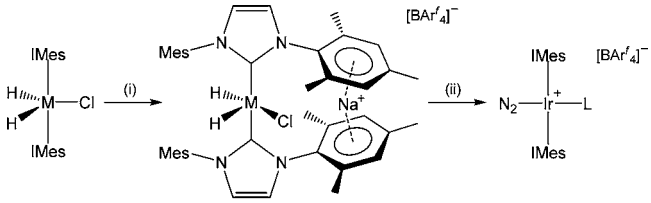

2: M = Rh
3: M = Ir
6: M = Rh
7: M = Ir
8a: L = N_2
8b: L = thf

[a] Key reagents and conditions: (i) Na[BAr$^f_4$], fluorobenzene, 3 h at 20°C, ca. 70%; (ii) dinitrogen atmosphere, toluene, 5 h at 80°C, recrystallization from either fluorobenzene (**8a**) or THF/pentane (**8b**), ca. 80%.

multinuclear NMR and elemental microanalysis is consistent with the proposed formulation for **5**, definitive establishment of connectivity was reliant on single crystal X-ray diffraction (Figure 1). The geometry of the cationic component of **5** is similar to that of the related square pyramidal complex [Ir(IPr′)(IPr″)H]$^+$ (Scheme 1) with each cation featuring a basal coordination plane composed of mutually *trans* NHC donors, alkene, and hydride/alkyl ligands;[11c] the apical coordination site is occupied by a hydride ligand in accordance with quantum chemical predictions for d^6 ML$_5$ systems.[27] In each case, the alkene moiety lies effectively parallel with the basal coordination plane (∠C(7)−Ir(1)−alkene centroid-C(3) = 178.5°, cf. 174.4° for the corresponding angle in [Ir(IPr′)(IPr″)H]$^+$); computational studies are consistent, however, with a relatively low lying alternative (perpendicular) ligand orientation (at +4.9 kcal mol^{-1} in the case of [Ir(IPr′)(IPr″)H]$^+$).[11c]

IMes Systems. Studies of systems stabilized by ancilliary IPr ligands reveal that although a bis(agostic)-stabilized species [Ir(IPr)$_2$(H)$_2$]$^+$ can be isolated from the reaction of **1** with Na[BAr$^f_4$], its subsequent reactivity toward B/N-containing systems is complicated by the presence of carbene substituents featuring β-hydrogen atoms. Dehydrogenation generates a tethered geminally disubstituted alkene function that competes with external donors for coordination at the iridium center. Thus, we targeted instead the related IMes complexes **2** and **3**, which although offering slightly reduced steric shielding of the metal center, also lack β-hydrogens within the carbene substituents. Surprisingly, the reaction of either **2** or **3** with Na[BAr$^f_4$] in fluorobenzene at 20 °C (under an argon atmosphere) does not proceed via salt metathesis but rather to the formation of the sodium-containing cations [M(IMes)$_2$(H)$_2$Cl(Na)]$^+$, (M = Rh, **6**; M = Ir, **7**) as the [BAr$^f_4$]$^-$ salts (Scheme 2).

Compounds **6** and **7** represent rare examples of isolated NaCl metathesis intermediates and can be shown to eliminate the metal halide in the presence of a suitable donor ligand (vide infra).[28] Both compounds have been characterized by standard spectroscopic techniques, by elemental microanalysis, and in the case of **7**, by single crystal X-ray diffraction. The cationic component of compound **7** in the solid state (Figure 2) is formally derived from **3** by intercalation of the sodium cation between the mesityl rings of the two IMes ligands. The Na−arene centroid distances characterizing these interactions

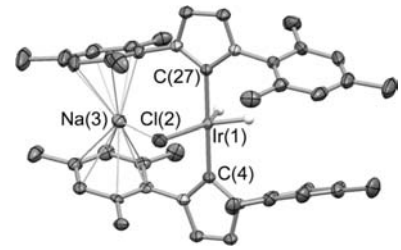

Figure 2. Molecular structure of the cationic component of **7**; hydrogen atoms (except those attached to the metal center) and second disorder component omitted for clarity. Thermal ellipsoids set at the 40% probability level. Key bond lengths (Å) and angles (deg): Ir(1)−Cl(2) 2.402(3), Cl(2)−Na(3) 2.612(7), C(4)−Ir(1)−C(27) 180 (by symmetry).

[2.456(7), 2.463(9) and 2.504(7) Å for **7** (allowing for the disorder)][29] are somewhat longer than those associated with other reported NaCl inclusion compounds [e.g., 2.145, 2.171 Å for Zn$_2$(ODipp)$_4$(Na)Cl(THF)$_3$].[30] That said, Zn$_2$(ODipp)$_4$-(Na)Cl(THF)$_3$ features a Na$^+$ cation bound to a *single* arene ring; comparison of **7** with related systems in which a sodium cation sits between two sterically encumbered π systems reveals that the Na−centroid distances and centroid−Na−centroid angle [143.7(3)°] are within the expected ranges (cf. 2.556, 2.535 Å and 150.7° for Na[(2,6-trip$_2$C$_6$H$_3$Ge)$_2$] (trip =2,4,6-^{i}Pr$_3$C$_6$H$_3$)).[31] Moreover, the presence of the sodium cation in **7** is also signaled by the effects it has on the conformation of the Ir(IMes)$_2$ unit; the two carbene heterocycles in **7** lie close to coplanar (torsion angle between least-squares planes =12.0°) in contrast to the more staggered geometry adopted by **3** (torsion = 47.5°),[10a] presumably on steric grounds.

Synthetically, **6** and **7** represent useful, highly reactive sources of the putative 14-electron cations [M(NHC)$_2$(H)$_2$]$^+$, readily eliminating NaCl in the presence of potential donors (vide infra). Although both compounds are stable under an argon atmosphere, the extremely facile loss of sodium chloride can readily be demonstrated by the isolation of the THF adduct [Rh(IMes)$_2$(H)$_2$(THF)]$^+$[BAr$^f_4$]$^-$ (see Supporting Information) and the fact that exposure of solutions of **7** to N_2 gas leads to the formation of related Ir(I) dinitrogen complexes, albeit with additional loss of H_2. Thus, heating of a toluene solution of **7** at 80 °C under a dinitrogen atmosphere for 5 h leads to the formation of [Ir(IMes)$_2$(N$_2$)$_2$]$^+$[BAr$^f_4$]$^-$ (**8a**) in ca. 80% yield after recrystallization from fluorobenzene. The closely related complex [Ir(IMes)$_2$(N$_2$)THF]$^+$[BAr$^f_4$]$^-$ (**8b**) is obtained in similar fashion after recrystallization from THF/pentane. Spectroscopic and microanalytical data for **8a** and **8b** are consistent with the proposed compositions; in particular N≡N stretching modes of vibration give rise to bands at 1993 and 1985 cm^{-1}, respectively. The structures of **8a** and **8b** have also been confirmed crystallographically (Figure 3) with each conforming to the planar four-coordinate geometry typical of d^8 Ir(I), and

(27) See, for example: (a) Rachidi, I. E.; Eisenstein, O.; Jean, Y. *New J. Chem.* **1990**, *14*, 671. (b) Riehl, J. F.; Jean, Y.; Eisenstein, O.; Pelissier, M. *Organometallics* **1992**, *11*, 729.

(28) For a previous example of an isolated metathesis intermediate see, for example: Patmore, N. J.; Ingelson, M. L.; Mahon, M. F.; Weller, A. S. *Dalton Trans.* **2003**, *289*, 4–2904.

(29) The crystal structure of **7** occupies a position on a 2-fold rotation axis such that one IMes and the sodium ion are disordered over two positions while the two halves of the second IMes are related by the symmetry operator. Thus there are three Na−centroid distances and two centroid−Na−centroid angles. Because the crystal structure is averaged over time and space, it is not possible to know the relationship between the disordered IMes and the sodium ion, however all distances and angles are given.

(30) Darensbourg, D. J.; Yoder, J. C.; Struck, G. E.; Holtcamp, M. W.; Draper, J. D.; Reibenspies, J. H. *Inorg. Chim. Acta* **1998**, *274*, 115–121.

(31) Pu, L.; Phillips, A. D.; Richards, A. F.; Stender, M.; Simons, R. S.; Olmstead, M. M.; Power, P. P. *J. Am. Chem. Soc.* **2003**, *125*, 11626–11636.

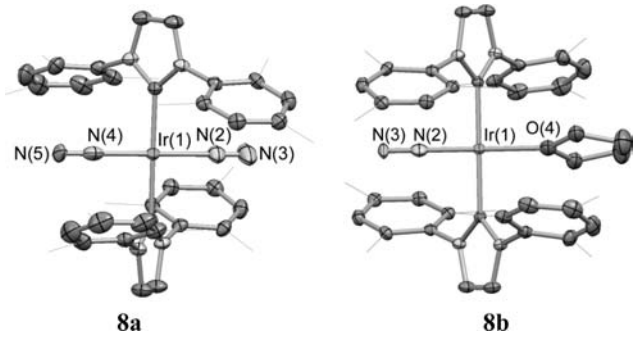

Figure 3. Molecular structures of the cationic components of **8a** and **8b**; hydrogen atoms and minor disorder component (for **8a**) omitted for clarity. Thermal ellipsoids set at the 40% probability level. Key bond lengths (Å) and angles (deg) for **8b**: Ir(1)−N(2) 1.840(6), N(2)−N(3) 1.109(8), Ir(1)−O(4) 2.128(5), Ir(1)−N(2)−N(3) 180.0 (by symmetry), N(2)−Ir(1)−O(4) 180.0 (by symmetry), C(7)−Ir(1)−C(7′) 179.7(2).

featuring *trans* NHC and *trans* N_2/N_2 or N_2/THF ligand pairs. Although the structure of complex **8a** represents, to our knowledge, the first such report of a bis(dinitrogen) complex of a group 9 metal, pernicious disorder prevents any meaningful discussion of bond metrics. However, the metrical parameters for **8b** [Ir−N and N−N distances of 1.840(6) and 1.109(8) Å, respectively] are similar to those reported for the related Ir(I) bis(phosphine) system *trans*-Ir(P^iPr_3)$_2$(N_2)Cl [1.822(10) and 1.028(14) Å] with the slightly longer N−N distance presumably reflecting, at least in part, the reduced degree of back-bonding from the cationic Ir(I) center in **8b**.[32]

As outlined above, a primary objective of this research program is an appraisal of the potential of $[(NHC)_2M(H)_2]^+$ systems for the coordination of B/N-containing substrates and their subsequent activation toward dehydrogenation chemistry. With this in mind, the reactions of **6** and **7** with primary, secondary, and tertiary amineboranes (i.e., $R_nH_{3-n}N\cdot BH_3$, $n = 1-3$) have been investigated.[33] While the latter class of compound (exemplified in the current studies by $Me_3N\cdot BH_3$) offers nothing in the way of dehydrogenation chemistry, initial studies sought to utilize this borane, not only to provide confirmation of the ability of the $[(IMes)_2M(H)_2]^+$ (M = Rh, Ir) fragments simply to bind B−H bonds but also as a basis for comparison (i) with other metal systems known to bind amineboranes, and (ii) with $[(IMes)_2M(H)_2]^+$ complexes containing dehydrogenated B/N ligand systems (vide infra). Accordingly, the reaction of $Me_3N\cdot BH_3$ with **6** or **7** in fluorobenzene leads to the formation of the 18-electron species $[M(IMes)_2(H)_2(\mu\text{-}H)_2B(H)\cdot NMe_3]^+[BAr^f{}_4]^-$ (M = Rh, **9**; M = Ir, **10**) in 68 and 75% isolated yields, respectively (Scheme 3). Spectroscopically, each complex is characterized in the ^{1}H NMR spectrum by two high field resonances with relative intensities 2:3 assigned to the M−H and (fluxional) B−H hydrogens, respectively [at δ_H −18.77, −1.27 for **9**; δ_H −21.80, −2.28 for **10**] and by a broad ^{11}B signal shifted slightly from that of the free borane, and which sharpens on broad-band ^{1}H decoupling (δ_B 1.5, 14.4, −7.3 for **9**, **10**, and $Me_3N\cdot BH_3$, respectively).[20o]

Scheme 3. Reactions of **6** and **7** with $Me_3N\cdot BH_3$; Formation of Simple η^2-Amineborane Adducts[a]

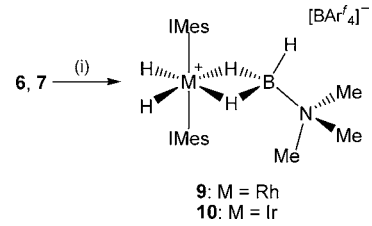

[a] Key reagents and conditions: (i) $Me_3N\cdot BH_3$ (20 equiv), fluorobenzene, 6 h at 20°C, 68% (for **9**), 75% (for **10**).

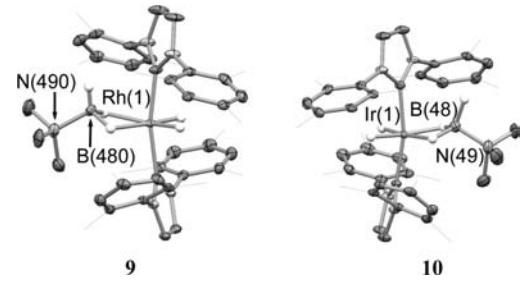

Figure 4. Molecular structures of the cationic components of **9** and **10**; hydrogen atoms (except those attached to metal and boron centers) omitted for clarity. Thermal ellipsoids set at the 40% probability level. Key bond lengths (Å) and angles (deg): (for **9**) Rh(1)···B(48) 2.327(3), B(48)−N(49) 1.605(5), Rh(1)···B(48)−N(49) 138.4(3), C(2)−Rh(1)−C(25) 166.6(1); (for **10**) Ir(1)···B(48) 2.230(2), B(48)−N(49) 1.581(1), Ir(1)···B(48)−N(49) 138.2(1), C(2)−Ir(1)−C(25) 166.6(2).

Structurally, **9** and **10** are each characterized by a pseudo-octahedral metal coordination geometry, featuring *trans* NHC, *cis* hydride ligands (which were visible in the difference map), and two additional hydrogens that constitute the points of attachment of a η^2-$Me_3N\cdot BH_3$ ligand (Figure 4). The B−N distances [1.605(5), 1.581(1) Å] and M···B−N angles [138.4(3), 138.2(2)°] for **9** and **10** are consistent with a coordinated ligand featuring four-coordinate boron and nitrogen centers. In each case the M···B distance [2.327(3) and 2.230(2) Å for **9** and **10**, respectively] is significantly longer than the sum of the respective covalent radii (2.13, 2.14 Å for Rh/B and Ir/B, respectively),[34] consistent with the presence of no significant direct M−B interaction and with the small change in δ_B on coordination of the borane.[20o] While significantly longer M···B distances have been reported for η^1-$Me_3N\cdot BH_3$ complexes (e.g., 2.648(3) Å for $[CpRu(PMe_3)_2(\mu\text{-}H)BH_2\cdot NMe_3]^+$),[35] that measured for an η^2-complex of $Me_2NH\cdot BH_3$ is very similar to that of **9** (2.318(8) Å for $[Rh(P^iBu_3)_2(H)_2(\mu\text{-}H)_2BH\cdot NMe_2H]^+$).[20k] Interestingly, the corresponding trimethylamineborane complex $[Rh(P^iBu_3)_2(H)_2(\mu\text{-}H)_2BH\cdot NMe_3]^+$ has been reported to be unstable with respect to loss of H_2 yielding the corresponding four-coordinate Rh(I) complex;[20k] by contrast no such spontaneous hydrogen loss is observed for the bis(IMes) system **9**, and indeed even in cases where such dehydrogenation chemistry

(32) (a) Werner, H.; Höhn, A. *Z. Naturforsch.* **1984**, *39b*, 1505. (b) Bottcher, H.-C.; Graf, M.; Mayer, P.; Suenkel, K. *Z. Anorg. Allg. Chem.* **2008**, *634*, 1241.

(33) The reactivity of **6** towards the parent B/N system ammonia borane, $H_3N\cdot BH_3$, in fluorobenzene has also been investigated. These studies are consistent with the formation of a mixture of dehydrogenated products and with the ultimate formation of the cationic donor/acceptor adduct $[(IMes)BH_2NH_3]^+$ (as the $[BAr^f{}_4]^-$ salt). Thus, although **6** *does* appear to catalyze the dehydrogenation of ammonia borane, its use in practice is limited by degradation processes involving ligand abstraction from the metal by strongly Lewis acidic borane species. Full spectroscopic, analytical and crystallographic data for $[(IMes)BH_2NH_3]^+$-$[BAr^f{}_4]^-$ are included in Supporting Information.

(34) Emsley, J. In *The Elements*; Oxford University Press: Oxford, 1991.

(35) (a) Shimoi, M.; Nagai, S.; Ichikawa, M.; Kawano, Y.; Katoh, K.; Uruichi, M.; Ogino, H. *J. Am. Chem. Soc.* **1999**, *121*, 11704–11712. (b) Kakizawa, T.; Kawano, Y.; Shimoi, M. *Organometallics* **2001**, *20*, 3211–3213. (c) Kawano, Y.; Hashiva, M.; Shimoi, M. *Organometallics* **2006**, *25*, 4420–4426. (d) Kawano, Y.; Yamaguchi, K.; Miyake, S.; Kakizawa, T.; Shimoi, M. *Chem.—Eur. J.* **2007**, *13*, 6920–6931.

Scheme 4. Synthesis of Aminoborane Complexes **11**−**14** by the Dehydrogenation of Secondary Amineboranes[a]

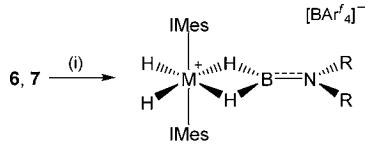

11: M = Rh, R = ^{i}Pr
12: M = Rh, R = Cy
13: M = Ir, R = ^{i}Pr
14: M = Ir, R = Cy

[a] Key reagents and conditions: (i) $R_2HN{\cdot}BH_3$ (20 equiv), fluorobenzene, 6 h at 20°C, 56−71%.

can be effected [e.g., by the addition of 3,3-dimethylbutene (*tert*-butylethylene, TBE)], subsequent C−H activation chemistry typically regenerates a six-coordinate metal complex (vide infra). As such, these empirical observations for rhodium systems point to the IMes ligand being somewhat less sterically demanding than P^{i}Bu$_3$.[36] To our knowledge, **10** represents the first example of an amineborane complex of iridium to be reported.

The corresponding reactions of **6** and **7** with systems containing N−H bonds (i.e., primary and secondary amineboranes) ultimately result in dehydrogenation of the BN moiety to give complexes containing unsaturated aminoborane ligands (Scheme 4). Thus, **6** and **7** catalyze the dehydrogenation of the secondary amineboranes $R_2HN{\cdot}BH_3$ (R = ^{i}Pr, Cy) in fluorobenzene at room temperature (100% conversion over 4 h at 2 mol % loading for **6**; synthetic runs typically performed at 5 mol %), leading to the generation of monomeric R_2NBH_2; the metal-containing products isolated on completion of these reactions (after recrystallization from fluorobenzene/hexanes) are the aminoborane adducts $[M(IMes)_2(H)_2(\mu\text{-}H)_2BNR_2)]^+$-$[BAr^f{}_4]^-$ [M = Rh, R = ^{i}Pr, **11**; M = Rh, R = Cy, **12**; M = Ir, R = ^{i}Pr, **13**; M = Ir, R = Cy, **14**]. The ^{11}B NMR resonances for all four cations (δ_B 35.4, 37.9, 35.8, and 35.9 ppm) are as expected for species containing three-coordinate boron centers formed by dehydrogenation of $R_2HN{\cdot}BH_3$ and indeed are very close to those of the free aminoboranes themselves (cf. δ_B 35.2, 35.4 for ^{i}Pr$_2$NBH$_2$ and Cy$_2$NBH$_2$).[20a,23,24] Moreover, the pattern of the ^{1}H NMR resonances in the hydride region in each case [e.g., δ_H −1.40 (2H), −16.02 (2H) for the B−H−Rh and Rh−H protons in **11**; cf. δ_H 4.32 for the B−H hydrogens of ^{i}Pr$_2$NBH$_2$ and −23.0 for rhodium-bound hydrides of Rh(IMes)$_2$(H)$_2$Cl],[20a,10a] provides evidence for coordination of the aminoborane to the $[M(IMes)_2(H)_2]^+$ fragment in solution. By means of comparison, the data reported for the high-field region of the ^{1}H NMR spectra of the related ruthenium η^2-boranes Ru(PCy$_3$)$_2$(H)$_2$(η^2-H$_2$BX) are δ_H −5.90, −11.05 (for X = Mes) and δ_H −6.80, −11.85 (for X = NH$_2$).[21,37,38] A subtle difference between **11** and **12** and these related charge-neutral ruthenium systems is the lower-field (less hydridic) chemical shift range observed for the B−H−M hydrogens (δ_H = −1.40, −1.74 ppm for **11** and **12**, respectively). This data, along with crystallographic evidence, is consistent with weaker binding of the borane fragment in the case of the cationic rhodium systems (vide infra).

Although NMR data are consistent with an interaction of the aminoborane molecule with the Group 9 metal center via bridging B−H−M interactions, the fluxional behavior and variable hapticity characteristic of many B−H containing ligand systems[39] means that definitive characterization of the mode of ligation was reliant on single crystal X-ray diffraction studies (Figure 5).

The structures of the cationic components of **11**−**14** each feature the expected *trans* arrangement of the NHC donors, *cis* hydride ligands (which were visible in the difference Fourier maps in each case), and an aminoborane ligand featuring a planar C_2NBH_2 skeleton coordinated to the metal center via two B−H−M interactions, i.e., acting as a bis(σ-borane) ligand.[21,37–39,41] The B−N distances [1.370(4), 1.379(8), 1.380 (mean) and 1.424(12) Å, respectively] are consistent with appreciable π bond character [cf. 1.58 Å for the sum of the respective covalent radii and 1.380(6) for the B−N separation in Ph_2NBCl_2].[34,42] Moreover the Rh···B separations for **11** and **12** [2.204(4) and 2.176 (mean) Å] are notably shorter than those measured for related rhodium complexes containing an *amine*borane ligand (i.e., featuring a four-coordinate boron center); the corresponding distances determined for **9** and **15** (vide infra) are 2.327(3) and 2.305(4) Å, respectively. In a similar fashion, the Ir−B distances measured for **12** and **14** [2.088(5) and 2.025(mean) Å] are markedly shorter than that measured for η^2-$Me_3N{\cdot}BH_3$ complex **10** [2.230(2) Å]. By contrast, the M···B distances determined for rhodium complexes **11** and **12** are markedly *longer* than those associated with η^2-borane complexes featuring the isoelectronic $[Ru(PCy_3)_2(H)_2]$ fragment.[21,37–39,41] In the case of these ruthenium systems, the presence of a direct Ru−B interaction has been suggested, reflecting ruthenium−boron separations [1.938(4), 1.934(2) and 1.956(2) Å for complexes of MesBH$_2$, ^{t}BuBH$_2$, and NH$_2$BH$_2$, respectively], which are up to 0.15 Å (7.2%) shorter than the sum of the respective covalent radii (2.09 Å).[21,34,37,38] In the cases of the isoelectronic rhodium cations **11** and **12**, however, the extent of any analogous M−B interaction is likely to be significantly smaller, as indicated (i) by M···B separations that are actually *longer* than the sum of the corresponding covalent radii (2.13 Å),[34] and (ii) by the relatively small shifts in the aminoborane ^{11}B NMR resonance on coordination in each case ($\Delta\delta_B$ < 3 ppm cf. $\Delta\delta_B$ 10 ppm for H$_2$B^{t}Bu on coordination at ruthenium).[40,43] Moreover, the longer M−-B distances measured for **11** and **12** are also consistent with the idea of more weakly bound borane ligands implied by the less hydridic Rh−H−B ^{1}H NMR resonances.

The bis(σ-borane) mode of coordination observed for aminoborane molecules bound to the $[M(IMes)_2(H)_2]^+$ fragment in **11**−**14** clearly contrasts with the classical side-on mode of binding typically observed for isoelectronic alkene donors toward transition metals.[5] Moreover, the structural data obtained for **5** confirm that a conventional side-on mode of binding of an alkene to the $[Ir(IPr)_2(H)_2]^+$ fragment is viable, with only slight asymmetry in the Ir−C distances [2.239(4) and 2.275(3)

(36) For a recent review examining comparative steric properties of tertiary phosphine and NHC ligands see, for example:Clavier, H.; Nolan, S. *Chem. Commun.* **2010**, *46*, 841–861.
(37) Alcaraz, G.; Clot, E.; Helmstedt, U.; Vendier, L.; Sabo-Etienne, S. *J. Am. Chem. Soc.* **2007**, *129*, 8704–8705.
(38) Alcaraz, G.; Helmstedt, U.; Clot, E.; Vendier, L.; Sabo-Etienne, S. *J. Am. Chem. Soc.* **2008**, *130*, 12878–12879.
(39) See, for example: Marks, T. J.; Kolb, J. R. *Chem. Rev.* **1977**, *77*, 263–293.
(40) (a) Gloaguen, Y.; Alcaraz, G.; Vendier, L.; Sabo-Etienne, S. *J. Organomet. Chem.* **2009**, *694*, 2839–2841. (b) Alcaraz, G.; Grellier, M.; Sabo-Etienne, S. *Acc. Chem. Res.* **2009**, *42*, 1640.
(41) Hesp, K. D.; Rankin, M. A.; McDonald, R.; Stradiotto, M. *Inorg. Chem.* **2008**, *47*, 7471–7473.
(42) Zettler, F.; Hess, H. *Chem. Ber.* **1975**, *108*, 2269–2273.
(43) For an analysis of the effects of metal-boron bonding on ^{11}B chemical shifts see, for example: Weller, A. S.; Fehlner, T. P. *Organometallics* **1999**, *18*, 447–450.

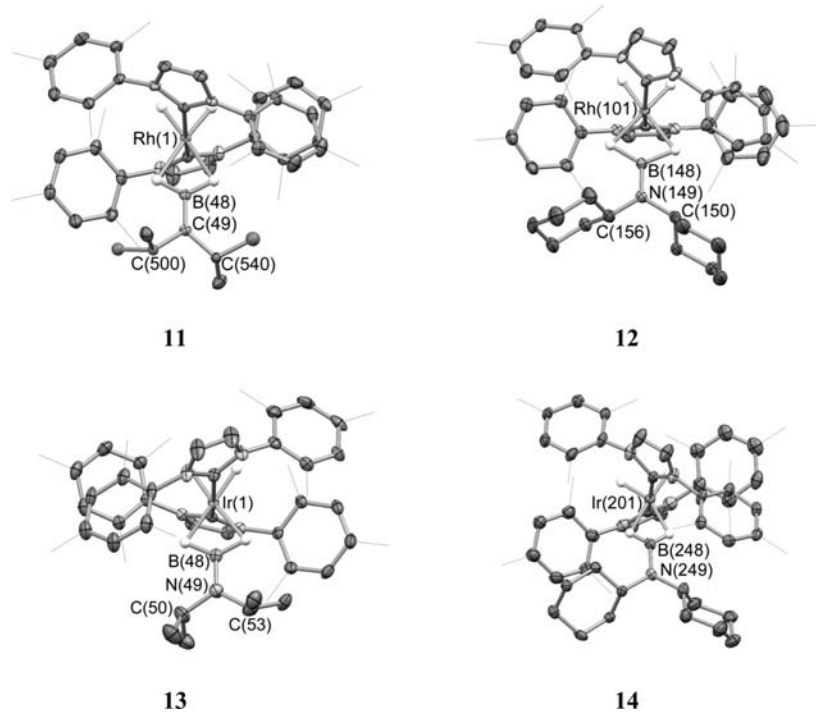

Figure 5. Molecular structures of the cationic components of **11** and **13**, and of one of the cationic components of the asymmetric unit of **12** and **14**; hydrogen atoms (except those attached to metal centers) omitted for clarity. Thermal ellipsoids set at the 40% probability level. Key bond lengths (Å) and angles (deg): (for **11**) Rh(1)···B(48) 2.204(4), B(48)−N(49) 1.370(4), Rh(1)−B(48)−N(49) 179.6(3), C(2)−Rh(1)−C(25) 165.5(1); (for **12**) Rh(101)···B(148) 2.198(7), B(148)−N(149) 1.380(8), Rh(101)···B(148)−N(149) 177.9(5), C(102)−Rh(101)−C(125) 161.4(2); (for **13**) Ir(1)···B(48) 2.088(5), B(48)−N(49) 1.379(8); Ir(1)−B(48)−N(49) 178.4(3), C(2)−Ir(1)−C(25) 165.6(2); (for **14**) Ir(201)···B(248) 2.027(10), B(248)−N(249) 1.424(12), Ir(201)···B(248)−N(249) 177.2(8), C(202)−Ir(201)−C(225) 164.8(3).

Å] reflecting closer approach of the less hindered terminal alkene carbon. It therefore seems likely that the alternative binding motif revealed for aminoboranes is reflective of the electronic properties of this type of ligand, and in particular the more hydridic nature of the B−H bonds (cf. C−H), and the significantly lower energy of the B═N π system (cf. C═C).[44] Consistent with this assertion, Alcaraz and Sabo-Etienne have reported that the end-on bis(σ-borane) binding motif is the most stable isomer of the model complex *trans*-Ru$(PMe_3)_2(H)_2$-(H_2BNH_2) with alternative modes of interaction utilizing the BN π system being >14 kcal mol^{-1} higher in energy.[21]

Similar dehydrogenation chemistry is applicable to the primary amineborane ^{t}BuNH$_2$·BH$_3$, although in this case the *rate* of rhodium-catalyzed dehydrogenation appears to be slower. Moreover, in common with the findings of Kawano, Shimoi and co-workers, the dehydrogenation of ^{t}BuNH$_2$·BH$_3$ under such conditions leads to the formation of a mixture of products, including $B_2H_5(\mu$-NH^{t}Bu), (^{t}BuNH)$_2$BH, ^{t}BuNHBH$_2$, and (^{t}BuN-BH)$_3$.[45] Not unexpectedly, the proportion of dehydrogenated B/N containing species (as measured by ^{11}B NMR spectroscopy) increases as a function of time; moreover from the perspective of the rhodium-containing species present in solution, short reaction times (ca. 6 h) lead to the isolation of the *amine*borane complex $[Rh(IMes)_2(H)_2(\mu\text{-}H)_2B(H)\cdot NH_2{}^tBu]^+[BAr^f{}_4]^-$ (**15**), while extended reaction times (ca. 48 h) bring about the formation of the corresponding (dehydrogenated) *amino*borane

Scheme 5. Isolation of Amine- and Aminoborane Complexes from the Complexation and Dehydrogenation of ^{t}BuNH$_2$·BH$_3$[a]

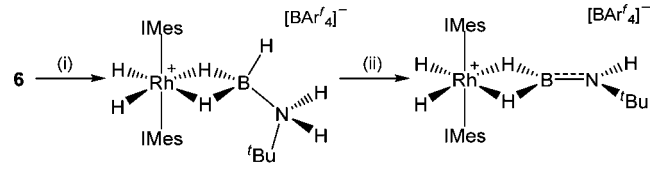

[a] Key reagents and conditions: (i) ^{t}BuH$_2$N·BH$_3$ (20 equiv), fluorobenzene, 6 h at 20°C, 51%; (ii) from **6**: ^{t}BuH$_2$N·BH$_3$ (20 equiv), fluorobenzene, 48 h at 20°C, 72%.

system $[Rh(IMes)_2(H)_2(\mu\text{-}H)_2BNH^tBu]^+[BAr^f{}_4]^-$ (**16**) (Scheme 5). **15** and **16** have been characterized by standard spectroscopic and analytical techniques, with the ^{11}B NMR chemical shifts for the coordinated boranes (δ_B −35.1, and 37.4, respectively) being particularly diagnostic of the coordination number at boron, and hence on the extent of hydrogenation of the coordinated borane fragment. The ^{1}H NMR resonance associated with the boron-bound hydrogens occurs at higher field for **16** (δ_H −2.62 cf. −1.66 ppm for **15**), consistent with η^2-ligated boranes in each case and with fluxional averaging of one B−H and two Rh−H−B protons in **15**. Crystallographic authentication of the η^2 mode of ligation has been achieved for both **15** and **16** (Figure 6); these structural studies allow, for the first time, comparison of a saturated amineborane and the corresponding unsaturated aminoborane coordinated to the same transition metal fragment, i.e., $[Rh(IMes)_2(H)_2]^+$.

The geometric differences between **15** and **16** associated with the coordinated B/N fragment are largely as expected on the basis of the lower coordination number at the boron and nitrogen centers, i.e., shorter B−N and Rh···B distances [1.368(7) vs

(44) Results derived from photoelectron spectroscopy imply that the BN π bonding orbital in $H_2N{=}H_2$ is stabilized by 0.85 eV (ca. 80 kJ mol^{-1}) with respect to the corresponding orbital in $H_2C{=}CH_2$. See: Westwood, N. P. C.; Westiuk, N. H. *J. Am. Chem. Soc.* **1986**, *108*, 891–894.

(45) Kawano, Y.; Uruichi, M.; Shimoi, M.; Taki, S.; Kawaguchi, T.; Kakizawa, T.; Ogino, H. *J. Am. Chem. Soc.* **2009**, *131*, 14946–14957.

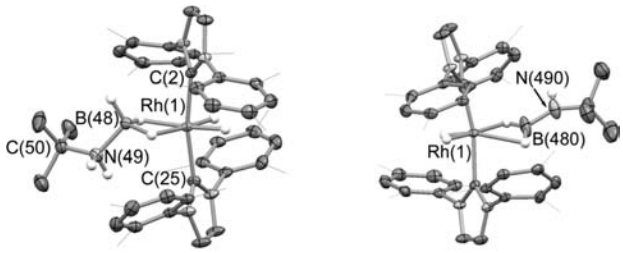

15 16

Figure 6. Molecular structures of the cationic components of **15** and **16**; hydrogen atoms (except those attached to metal centers) and minor disorder component (for **16**) omitted for clarity. Thermal ellipsoids set at the 40% probability level. Key bond lengths (Å) and angles (deg): (for **15**) Rh(1)···B(48) 2.305(4), B(48)−N(49) 1.604(5), Rh(1)···B(48)−N(49) 127.0(3), C(2)−Rh(1)−C(25) 168.7(1); (for **16**) Rh(1)···B(480) 2.245(7), B(480)−N(490) 1.368(7), Rh(1)···B(480)−N(490) 152.7(4), C(2)−Rh(1)−C(25) 168.1(2).

1.604(5) Å; 2.245(7) vs 2.305(4) Å] and a wider Rh···B−N angle [152.7(4) vs 127.0(3)°] for the aminoborane complex **16**. That said, the geometry of the $[Rh(IMes)_2(H)_2]^+$ fragment does not appear to vary significantly between the two complexes [d(Rh−C_{NHC}) = 2.044(3), 2.051(4) and 2.043(3), 2.045(3); ∠(C_{NHC}−Rh-C_{NHC}) = 168.7(1), 168.1(2)°, for **15** and **16** respectively], implying that the pocket available for the coordination of additional ligands is sufficient to accommodate both the planar aminoborane ligand and the more bulky amineborane. Such a finding contrasts with results reported for related systems containing a bis(triisobutylphosphine) ligand set, in which case coordination of bulkier amineboranes induces reductive elimination of H_2 from the metal center in order to relieve steric crowding.[20k,o] Indeed, in the case of the $[M(IMes)_2(H)_2]^+$ systems reported here, further loss of dihydrogen can only be effected by the addition of a sacrificial alkene such as *tert*-butylethylene. In the case of iridium dicyclohexylaminoborane system **14**, loss of H_2 is revealed by the generation of *tert*-butylethane but is also accompanied by oxidative addition of one of the IMes methyl C−H bonds to give $[Ir(IMes)(IMes')(H)(\mu\text{-}H)_2BNCy_2]^+[BAr^f{}_4]^-$ (**17**; Scheme 6).

The identity of **17** has been deduced from standard spectroscopic and analytical techniques, with additional confirmation being provided by X-ray diffraction (Figure 7). Structurally, the geometry of the Ir(μ-H)$_2$BNCy$_2$ unit varies little from that determined for complex **14**, with the Ir···B distances being statistically indistinguishable [2.012(8) vs 2.027(10) Å for **14**]. The structure of **17** is indicative of an alternative response to the unsaturation brought about by loss of H_2 from six-coordinate 18-electron σ-borane complexes, contrasting with the simple change in metal coordination geometry revealed by Weller and Hall for Rh(P^{i}Bu$_3$)$_2$ systems and the borane to borylene conversion reported by Sabo-Etienne and Alcaraz for Ru(PCy$_3$)$_2$ complexes, each of which involves a change in the formal oxidation state either of the metal or of the boron ligand.[20k,38]

Interestingly **17** can be further dehydrogenated under more forcing conditions to give complex **18**, which features a direct Ir−B interaction, as revealed by a short Ir−B distance, similar to that expected for an Ir═B double bond [1.881(8), cf. 1.892(3) for the iridium aminoborylene complex Cp*Ir(CO)═BN(SiMe$_3$)$_2$ and 2.012(8) Å for **17**].[46] Closer inspection, however reveals that the Ir−B−N framework is distorted somewhat from linearity [∠Ir−B−N = 167.2(6) cf. 175.9(3)° for Cp*Ir(CO)═BN(SiMe$_3$)$_2$] and that a bridging hydrogen atom between Ir(1) and B(48) is visible in the difference Fourier map with Ir−H and B−H distances [d(Ir−H) = 1.613(8), d(B−H) = 1.343 Å (riding)] consistent with other Ir(μ-H)B motifs [e.g., 1.81 Å (mean) and 1.32 Å (mean) for **17**]. Further evidence for the presence of H(481) and for some degree of direct B−H interaction can also be obtained from ^{11}B and ^{1}H NMR measurements. The ^{11}B resonance for **18** (δ_B 38.0 ppm) is at much higher field than typical aminoborylene complexes [cf. δ_B 67 ppm for Cp*Ir(CO)═BN(SiMe$_3$)$_2$],[46,47] and the only high field ^{1}H NMR resonance (at δ_H −10.85 ppm) falls intermediate between the Ir−H and Ir−H−B signals for **14** (δ_H −15.44 and −5.83 ppm, respectively); moreover, this ^{1}H signal narrows markedly on ^{11}B decoupling. As such, it seems likely that the structure of **18** can be described in terms of significant contributions from two limiting resonance forms, i.e., an iridium borylene complex stabilized by intramolecular B-coordination of an iridium-bound hydride or an α-agostic iridium boryl system (Scheme 7). Consistent with this description, the atoms Ir(1), H(481), B(48), and N(49), together with tertiary carbons of the cyclohexyl groups [C(50) and C(56)] are approximately coplanar, with the largest out-of-plane deviation being <0.07 Å. Interestingly, the bridging position of the hydride ligand in **18** implied by NMR and crystallographic measurements, contrasts with that reported for a related ruthenium system, which is described in terms of noninteracting hydride and borylene ligands within an isoelectronic (but charge-neutral) $L_2Ru(X)H(BR)$ system.[38] Conceivably this reflects the greater electrophilicity of the boron center within cationic borylene systems such as **18**.[47] However, precedent for this type of bridging interaction within strongly electrophilic cations such as **18** comes from the structure of [Cp*Mo(dmpe)(H)SiMes]$^+$ reported by Mork and Tilley.[48]

Quantum chemical studies of the mechanism of secondary amineborane dehydrogenation at Group 9 metal centers have recently been reported, albeit for less bulky systems in which the dehydrogenated aminoborane species ultimately couple to give oligomeric products;[20k] notably, the binding energies of $Me_2HN{\cdot}BH_3$ and (monomeric) Me_2NBH_2 at cationic 14-electron metal centers are reported not to be markedly different. In systems where the dehydrogenated aminoborane product has a more limited propensity to oligomerize [as with R_2NBH_2 (R = Cy, ^{i}Pr) and to a lesser extent ^{t}BuNHBH$_2$], the identities of the metal/boron-containing products isolated after different time periods are therefore (at least in part) reflective of the relative concentrations of the starting amineborane and dehydrogenated aminoborane present in solution. Thus, the underlying reasons for the different products obtained in the reactions of **6**/**7** with ^{t}Bu$H_2N{\cdot}BH_3$ and $R_2HN{\cdot}BH_3$ (R = ^{i}Pr, Cy) appear to reflect the relative rates of metal-catalyzed dehydrogenation of these amineboranes in fluorobenzene and consequently the identities of the predominant B/N-containing species in solution (at the end of the 6 h reaction period) available to coordinate to the $[M(IMes)_2(H)_2]^+$ fragment. Thus, whereas $R_2HN{\cdot}BH_3$ (R = ^{i}Pr, Cy) is efficiently dehydrogenated by **6** over the time-period of the synthetic experiment (6 h), effectively leaving R_2NBH_2 (R = ^{i}Pr, Cy) as the only borane remaining in solution, ^{t}Bu$H_2N{\cdot}BH_3$ is dehydrogenated much more slowly, such that over the same time frame it remains a major B/N constituent

(46) Braunschweig, H.; Forster, M.; Kupfer, T.; Seeler, F. *Angew. Chem., Int. Ed.* **2008**, *47*, 5981.
(47) (a) Braunschweig, H.; Kollann, C.; Seeler, F. *Struct. Bonding (Berlin)* **2008**, *130*, 1. (b) Vidovic, D.; Pierce, G. A.; Aldridge, S. *Chem. Commun.* **2009**, 1157. (c) Braunschweig, H.; Dewhurst, R. D.; Schneider, A. *Chem. Rev.* Published ASAP March 17, 2010, DOI:, 10.1021/cr900333n.
(48) Mork, B. V.; Tilley, T. D. *Angew. Chem., Int. Ed.* **2003**, *42*, 357.

Scheme 6. Dehydrogenation and C−H Activation in Aminoborane Complex **14**[a]

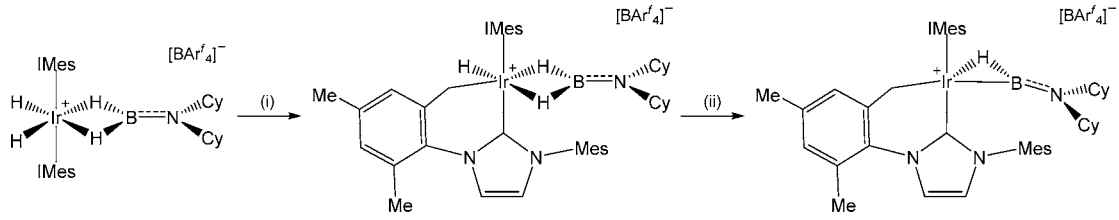

[a] Key reagents and conditions: (i) 3,3-dimethylbutene (TBE; excess), fluorobenzene, 6 h at 20°C, 63%; (ii) toluene, 36 h at 65°C, 82%.

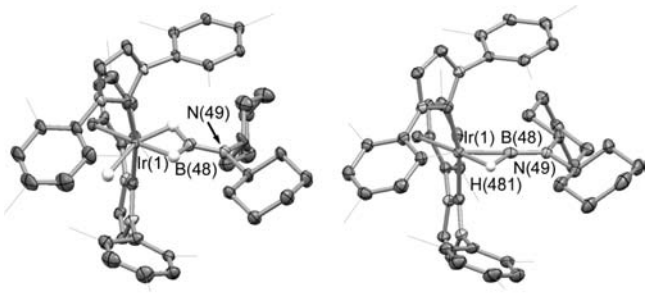

Figure 7. Molecular structure of the cationic components of **17** and **18**; hydrogen atoms (except those attached to the metal center) omitted for clarity. Thermal ellipsoids set at the 40% probability level. Key bond lengths (Å) and angles (deg): (for **17**) Ir(1)···B(48) 2.012(8), B(48)−N(49) 1.365(9), Ir(1)···B(48)−N(49) 168.4(5), C(6)−Ir(1)−C(25) 167.6(2); (for **18**) Ir(1)−B(48) 1.881(8), B(48)−N(49) 1.372(10), Ir(1)−H(481) 1.613(8), B(48)−H(481) 1.343 (riding), Ir(1)−B(48)−N(49) 167.2(6), C(2)−Ir(1)−C(29) 168.1(2).

Scheme 7. Limiting Valence Bond Descriptions of Complex **18**

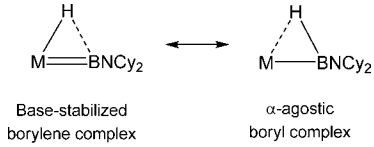

of the reaction mixture. Consistent with this assertion, extension of the reaction period in the case of ^{t}BuH$_2$N·BH$_3$ dehydrogenation leads to larger concentrations of the monomeric aminoborane ^{t}BuNHBH$_2$ in solution (as judged by in situ ^{11}B NMR spectroscopy) and to the isolation of [Rh(IMes)$_2$(H)$_2$(μ-H)$_2$BNH^{t}Bu]$^+$[BAr$^f_4$]$^-$ (**16**) after ca. 48 h.

Conclusions

Chloride abstraction from the Group 9 metal bis(N-heterocyclic carbene) complexes M(NHC)$_2$(H)$_2$Cl has been shown to generate highly reactive cationic species capable of the dehydrogenation of saturated CC and BN linkages. Thus, the reaction of Ir(IPr)$_2$(H)$_2$Cl (**1**) with Na[BAr$^f_4$] in fluorobenzene generates [Ir(IPr)$_2$(H)$_2$]$^+$[BAr$^f_4$]$^-$ (**4**) in which the iridium center is stabilized by a pair of agostic interactions; subsequent C−H activation leads to the dehydrogenation of one of the carbene ^{i}Pr substituents and the formation of [Ir(IPr)(IPr″)(H)$_2$]$^+$[BAr$^f_4$]$^-$ (**5**), featuring the mixed NHC/alkene donor IPr″ ligand. The closely related IMes complexes M(IMes)$_2$(H)$_2$Cl (M = Rh, Ir), which feature carbene substituents lacking β-hydrogens, react with Na[BAr$^f_4$] in fluorobenzene to give rare examples of NaCl inclusion compounds [M(IMes)$_2$(H)$_2$Cl(Na)]$^+$[BAr$^f_4$]$^-$ (M = Rh, **6**; M = Ir, **7**); crystallographic studies of **7** reveal intercalation of the sodium cation between the mesityl aromatic rings of the two NHC donors. Compounds **6** and **7** represent convenient yet highly reactive sources of the putative 14-electron [M(NHC)$_2$(H)$_2$]$^+$ cations, readily eliminating NaCl in the presence of potential donors. Thus **7** can be employed in the synthesis of the dinitrogen complexes [Ir(IMes)$_2$(N$_2$)$_2$]$^+$[BAr$^f_4$]$^-$ (**8a**) and [Ir(IMes)$_2$(N$_2$)THF]$^+$[BAr$^f_4$]$^-$ (**8b**) (albeit with additional loss of H$_2$) by simple dissolution in fluorobenzene or THF under a dinitrogen atmosphere. The reactivity of **6** and **7** toward primary, secondary, and tertiary amineboranes have also been investigated; reaction with the latter class of reagent leads to simple coordination of the amineborane at the metal center via two M−H−B bridges and the formation of [M(IMes)$_2$(H)$_2$(μ-H)$_2$B(H)·NMe$_3$]$^+$[BAr$^f_4$]$^-$ (M = Rh, **9**; M = Ir, **10**). The corresponding reactions with systems containing N−H bonds proceed via dehydrogenation to give complexes of the corresponding (unsaturated) aminoborane ligands. Thus, for example, **6** catalyzes the dehydrogenation of R$_2$HN·BH$_3$ (R = ^{i}Pr, Cy) in fluorobenzene solution to give [Rh(IMes)$_2$(H)$_2$(μ-H)$_2$BNR$_2$]$^+$[BAr$^f_4$]$^-$ (R = ^{i}Pr, **11**; R = Cy, **12**) as the ultimate organometallic products. In contrast to isoelectronic alkene donors, the aminoborane ligand in these complexes (and in the corresponding iridium compounds **13** and **14**) can be shown by crystallographic methods to bind in end-on fashion via a bis(σ-borane) motif. Similar dehydrogenation chemistry is applicable to the primary amineborane ^{t}BuH$_2$N·BH$_3$, although in this case the *rate* of rhodium-catalyzed dehydrogenation is slower, thereby allowing the *amine*borane complexes [Rh(IMes)$_2$(H)$_2$(μ-H)$_2$B(H)·NH$_2$^{t}Bu]$^+$[BAr$^f_4$]$^-$ (**15**) to be isolated at short reaction times (ca. 6 h) and the corresponding (dehydrogenated) aminoborane systems [Rh(IMes)$_2$(H)$_2$(μ-H)$_2$BNH^{t}Bu]$^+$[BAr$^f_4$]$^-$ (**16**) to be isolated after an extended period (ca. 48 h). Reactivity-wise aminoborane systems such as **14** show themselves to be amenable to further dehydrogenation chemistry, leading initially to intramolecular C−H activation processes, but ultimately to the dehydrogenation of the boron-containing ligand itself and to the formation of a system described by limiting boryl (Ir−B) and borylene (Ir═B) forms.

Acknowledgment. We thank the EPSRC for support of this work (EP/F01600X/1). We also gratefully thank the Diamond Light Source for an award of beam-time on I19 (MT1880) and the instrument scientists on the beamline for technical assistance.

Supporting Information Available: Synthetic, spectroscopic and crystallographic data for [(IMes)BH$_2$NH$_3$]$^+$[BAr$^f_4$]$^-$; crystallographic data for [Rh(IMes)$_2$(H)$_2$(THF)]$^+$[BAr$^f_4$]$^-$. This material is available free of charge via the Internet at http://pubs.acs.org.

JA1043787